Frequency domain homogenization for the viscoelastic properties of spatially correlated quasi-periodic lattices

T. Mukhopadhyay [a],[*], S. Adhikari [b], A. Batou [c]

[a] *Department of Engineering Science, University of Oxford, Oxford, UK*
[b] *College of Engineering, Swansea University, Swansea, UK*
[c] *Liverpool Institute for Risk and Uncertainty, University of Liverpool, Liverpool, UK*

A B S T R A C T

An analytical framework is developed for investigating the effect of viscoelasticity on irregular hexagonal lattices. At room temperature many polymers are found to be near their glass temperature. Elastic moduli of honeycombs made of such materials are not constant, but changes in the time or frequency domain. Thus consideration of viscoelastic properties are essential for such honeycombs. Irregularity in lattice structures being inevitable from practical point of view, analysis of the compound effect considering both irregularity and viscoelasticity is crucial for such structural forms. On the basis of a mechanics based bottom-up approach, computationally efficient closed-form formulae are derived in frequency domain. The spatially correlated structural and material attributes are obtained based on Karhunen–Loève expansion, which is integrated with the developed analytical approach to quantify the viscoelastic effect for irregular lattices. Consideration of such spatially correlated behaviour can simulate the practical stochastic system more closely. The two effective complex Young's moduli and shear modulus are found to be dependent on the viscoelastic parameters, while the two in-plane effective Poisson's ratios are found to be independent of viscoelastic parameters and frequency. Results are presented in both deterministic and stochastic regime, wherein it is observed that the amplitude of Young's moduli and shear modulus are significantly amplified in the frequency domain. The response bounds are quantified considering two different forms of irregularity, randomly inhomogeneous irregularity and randomly homogeneous irregularity. The computationally efficient analytical approach presented in this study can be quite attractive for practical purposes to analyse and design lattices with predominantly viscoelastic behaviour along with consideration of structural and material irregularity.

© 2017 Elsevier Ltd. All rights reserved.

Contents

* Corresponding author.
  E-mail address: tanmoy.mukhopadhyay@eng.ox.ac.uk (T. Mukhopadhyay).
  URL: http://www.tmukhopadhyay.com (T. Mukhopadhyay)

1. Introduction

Hexagonal lattices/lattice-like structural forms are present as materials and structures in abundance across various length-scales (nano, micro and macro) within natural systems and artificial products. Such structures have received considerable attention in last few decades as an advanced material because of the capability to meet high performance application-specific demands in various critically desirable parameters such as specific strength and stiffness, crushing resistance, fatigue strength, acoustic properties, shock absorption properties, electromechanical properties, corrosion and fire resistance [27]. The application of honeycomb core for lightweight sandwich structures is an active area of research [18,61,88,89]. An in-depth understanding of the structural behaviour of such hexagonal lattices is useful in emerging research fields of nano-materials like Graphene and Boron Nitride, which are often idealized as hexagonal periodic structures [50,65,73].

To eliminate the need of detail finite element modelling for hexagonal lattices/honeycombs as a part of another complex structural system (host structure such as sandwich panel), such lattices are generally modelled as a continuous solid medium with equivalent elastic moduli throughout the domain. A similar approach is followed to evaluate the effective material properties of different nano-structures having hexagonal configurations [65,66]. It is a common practice to consider a representative unit cell to model various other periodic structures [36]. Extensive research has been conducted so far to predict effective elastic properties of regular hexagonal lattices without any form of irregularity [23,27,31,53,90]. Computational homogenization techniques are reported in scientific literature to characterize the linear and non-linear responses of different lattices [7,69,70,76–79]. Other crucial research areas concerning different responses related to honeycombs include crushing behaviour, low velocity impact, buckling analysis and wave propagation through lattices [29,30,32,35,37,41,46,82,87,94]. Substantial amount of scientific literature is available dealing with perfectly periodic hexagonal auxetic lattices [6,14]. Recently theoretical formulations have been presented for equivalent elastic properties of periodic asymmetrical honeycomb [11]. Tailorable elastic properties of hierarchical honeycombs and spiderweb honeycombs have also been reported [3,57,72]. Analysis of two dimensional hexagonal lattices/honeycombs, as presented in the above literature review, are based on a unit cell approach, which can be applied only for perfectly periodic lattice forms.

The major limitation of the aforementioned unit cell based approach is that it cannot be used to analyse a system with spatial irregularity. Spatial irregularity/variability in lattices is practically inevitable; it may occur due to structural defects, manufacturing uncertainty, variation in temperature, micro-structural variability and pre-stressing. Moreover, development of novel meta-materials [83] having hexagonal microstructures may involve spatially varying structural and material attributes. To consider the effect of irregularity in cellular lattices, voronoi honeycombs are found to be considered in literature [44,92,93]. Dynamic crushing of honeycombs with irregularity in cell wall thickness and cell shapes have been investigated [45]. [84] have studied the failure surface of aluminium honeycombs for general inplane loading considering micro-structural imperfections. Papka and Kyriakides [74], [75] and Jang and Kyriakides [35] have reported numerical and experimen-

tal study of honeycomb crushing and buckling behaviour accounting for geometrical imperfections, such as over/ under expanded cells and variation in length of bond line. Ronan et al. [80] have recently investigated the tensile ductility of cellular solids including the effect of irregularity. The effect due to defects on regular as well as voronoi honeycombs and the effect of manufacturing uncertainty on auxetic honeycomb have been reported by Ajdari et al. [4] and Liu et al. [49], respectively. Though the above mentioned studies substantially investigate the effect of irregularities based on limited number of expensive samples, there is a further need to extend these works following a more realistic and robust probabilistic framework for spatially random imperfections/irregularities in order to develop appropriate uncertainty quantification models. For voronoi honeycombs, the shape of all the irregular cells may not be necessarily hexagonal that violates the presumption of hexagonal cell structure. A thorough review of the literature on hexagonal lattices/honeycomb dealing with different forms of structural irregularity reveals that the investigations are commonly based on either expensive finite element (FE) simulations or experimental investigations. As experimental investigations are expensive and time consuming, it is practically not feasible to quantify the effect of random irregularities in lattice structures by testing a huge number of samples. In the finite element approach, a small change in the geometry of a constituent cell may require completely new mesh generation. For dynamic and quasi-static analysis, separate finite element modelling of the honeycomb core in a sandwich structure may increase the degrees of freedom for the entire system up to such an extent that can make the overall process unmanageably complex and prohibitively expensive for simulation. In case of uncertainty quantification using a Monte Carlo based approach, the problem aggravates as large number of expensive finite element simulations are needed to be carried out [17,19–22,34,52,58,64,67,68]. Application of surrogate based approaches to achieve computational efficiency, as adopted in many of these papers, does not make the analysis physically insightful and this approach often suffer from lack of confidence in the predicted results. Surrogate based approaches may not perform well in case of high non-linearity in the model and high dimensional input parameter space, which becomes a crucial factor in analysing spatially irregular lattices. Moreover, large scale numerical simulation to quantify the effect of irregularity in cellular lattices may not necessarily yield proper understanding of the underlying physics of the system. An analytical approach for this purpose could be a simple, efficient, yet insightful alternative.

Recently an analytical framework has been reported for in-plane elastic moduli of hexagonal honeycombs with spatially varying structural configurations [59,60,62,63] without any spatial correlation. However, in practical situation the material and structural attributes are often found to be spatially correlated. Thus it is important to account for such correlation in structural irregularity and material property distribution. Moreover, many polymers are found to be near their glass temperature at room temperature. Elastic moduli of honeycombs made of such materials are not constant, but changes in the time or frequency domain. So consideration of viscoelastic properties are essential for such honeycombs. Gibson and Ashby [27] have provided analytical expressions for regular viscoelastic honeycombs in time domain. Otherwise, investigation on the viscoelastic properties of honeycomb-like lattices is very scarce to find in literature. Irregularity in lattice structures being inevitable from practical point of view, analysis of the compound
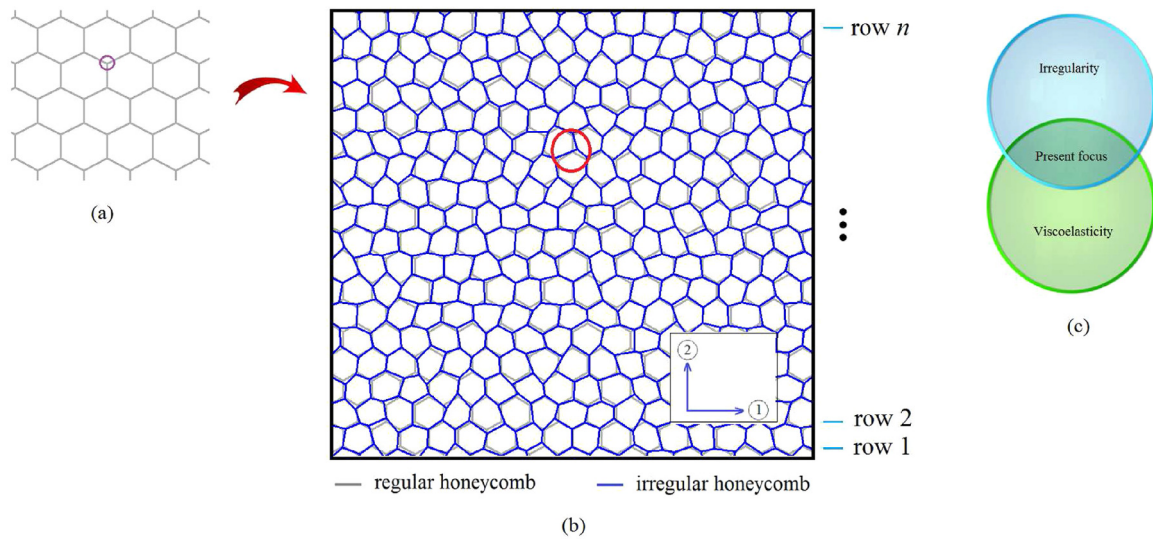
Fig. 1. (a) Illustration to define degree of irregularity and perturbation of nodes (b) Typical representation of irregular honeycomb (c) Scope and focus of the present study (d) Conventional unit cell for regular lattices (e) Representative unit cell element (RUCE) for the analysis of spatially irregular lattices.

effect considering both irregularity and viscoelasticty is crucial for such structural forms.

In the present paper, we aim to develop an analytical model to analyse spatially correlated irregular lattices considering viscoelastic properties in frequency domain (refer to Fig. 1(c)). The spatially correlated structural and material attributes are obtained based on Karhunen–Loève expansion, which is integrated with the developed analytical approach to quantify the viscoelastic effect. This paper deals with the viscoelastic properties of randomly disordered lattice structures that varies spatially i.e. the structural units are different in geometry along a two-dimensional plane; but they do maintain a particular shape. One representative unit in the present problem may be considered as shown in Fig. 1(e) and the entire lattice structure shown in Fig. 1(b) is basically a tessellation of the shape shown in Fig. 1(e) with different values of the lengths of the three members and their orientations. Thus such repetition of the representative units can be referred as quasi-periodicity. This article is organized hereafter as follows: description of the underlying concepts of viscoelastic analysis is provided in Section 2; derivation of the effective viscoelastic properties of irregular lattices is given in Section 3; effective viscoelastic properties of irregular lattices with correlated structural and material attributes based on Karhunen-Loève expansion is described in Section 4; Section 5 presents the numerical results based on the developed analytical formulae; Finally, Section 6 presents the conclusion and perspective of this paper.

2. Formulation for viscoelastic analysis

In classical elasticity, instantaneous stress within a material is a function of instantaneous strain only. In contrast, in viscoelasticity, instantaneous stress is considered to be a function of strain history. When a linear viscoelastic model is employed, the stress at some point of a structure can be expressed as a convolution integral over a kernel function [25] as

$$\sigma(t) = \int_{-\infty}^{t} g(t-\tau)\frac{\partial \epsilon(\tau)}{\partial \tau}\, d\tau \tag{1}$$

Here $t \in \mathbb{R}^+$ is the time, $\sigma(t)$ is stress and $\epsilon(t)$ is strain. The kernel function $g(t)$ also known as 'hereditary function', 'relaxation function' or 'after-effect function' in the context of different subjects. The stress-strain relationship in (1) can be directly applied to dynamic analysis of a solid body. For example, if it is applied to a uniform rod, Eq. (1) can be multiplied by the area and the equation can be expressed in terms of the force and displacement rate (or velocity). In practice, the kernel function is often defined in the frequency domain (or Laplace domain). Taking the Laplace transform of Eq. (1), we have

$$\bar{\sigma}(s) = s\bar{G}(s)\bar{\epsilon}(s) \tag{2}$$

Here $\bar{\sigma}(s)$, $\bar{\epsilon}(s)$ and $\bar{G}(s)$ are Laplace transforms of $\sigma(t)$, $\epsilon(t)$ and $g(t)$ respectively and $s \in \mathbb{C}$ is the (complex) Laplace domain parameter. There are two broad ways by which the kernel function $g(t)$ can be constructed, namely by a physics based approach or a more general mathematical approach.
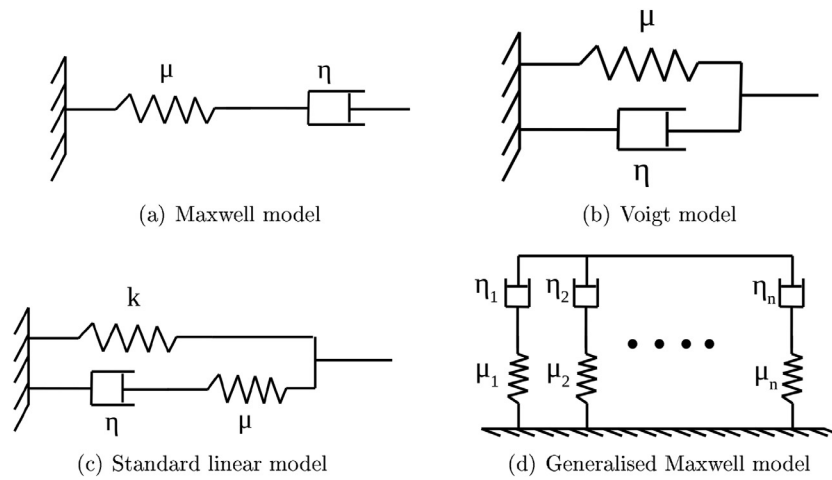
(a) Maxwell model   (b) Voigt model

(c) Standard linear model   (d) Generalised Maxwell model

Fig. 2. Springs and dashpots based models viscoelastic materials.

2.1. Physics-based representation of the kernel function

In a physics based approach, the kernel function appearing in the viscoelastic constitutive relationship can arise from a combination of springs and dashpots. This can be achieved in various ways. Four main cases are in shown in Fig. 2.

We define the unit step function $\mathcal{U}(t)$ and Dirac delta function $\delta(t)$ as below

$$\mathcal{U}(t) = \begin{cases} 1 & \text{if } t \geq 0, \\ 0 & \text{if } t < 0. \end{cases} \quad \text{and} \quad \delta(t) = \begin{cases} 0 & \text{if } t \neq 0, \\ \int_{-\infty}^{\infty} \delta(t)\mathrm{d}t = 1 \end{cases} \quad (3)$$

Using these functions, the viscoelastic kernel function can be expressed [10,13,25,38] for the four models as

- *Maxwell model:*

$$g(t) = \mu e^{-(\mu/\eta)t} \mathcal{U}(t) \quad (4)$$

- *Voigt model:*

$$g(t) = \eta \delta(t) + \mu \mathcal{U}(t) \quad (5)$$

- *Standard linear model:*

$$g(t) = E_R \left[1 - (1 - \frac{\tau_\sigma}{\tau_\epsilon}) e^{-t/\tau_\epsilon} \right] \mathcal{U}(t) \quad (6)$$

- *Generalised Maxwell model:*

$$g(t) = \left[\sum_{j=1}^{n} \mu_j e^{-(\mu_j/\eta_j)t} \right] \mathcal{U}(t) \quad (7)$$

Models similar to this is also known as the Prony series model.

These functions can be constructed by considering the equilibrium of forces arising by stretching the springs and dashpots appearing in Fig. 2.

2.2. Mathematical representation of the kernel function

The kernel function in Eq. (2) is a complex function in the frequency domain. For notational convenience we denote

$$\bar{G}(s) = \bar{G}(\mathrm{i}\omega) = G(\omega) \quad (8)$$

where $\omega \in \mathbb{R}^+$ is the frequency. The complex modulus $G(\omega)$ can be expressed in terms of its real and imaginary parts or in terms of its amplitude and phase as follows

$$G(\omega) = G'(\omega) + \mathrm{i}G''(\omega) = |G(\omega)|e^{\mathrm{i}\phi(\omega)} \quad (9)$$

The real and imaginary parts of the complex modulus, that is, $G'(\omega)$ and $G''(\omega)$ are also known as the storage and loss moduli respectively. One of the main restriction on the form of the kernel function comes from the

fact that the response of the structure must start before the application of the forces. This causality condition imposes a mathematical relationship between real and imaginary parts of the complex modulus, known as Kramers–Kronig relations (see for example [81] for recent discussions). Kramers–Kronig relations specifies that the real and imaginary parts should be related by a Hilbert transform pair, but can be general otherwise. Mathematically this can be expressed as

$$G'(\omega) = G_\infty + \frac{2}{\pi} \int_0^\infty \frac{uG''(u)}{\omega^2 - u^2} \mathrm{d}u$$

$$G''(\omega) = \frac{2\omega}{\pi} \int_0^\infty \frac{G'(u)}{u^2 - \omega^2} \mathrm{d}u \quad (10)$$

where the unrelaxed modulus $G_\infty = G(\omega \to \infty) \in \mathbb{R}$. Equivalent relationships linking the modulus and the phase of $G(\omega)$ can be expressed as

$$\ln |G'(\omega)| = \ln |G_\infty| + \frac{2}{\pi} \int_0^\infty \frac{u\phi(u)}{\omega^2 - u^2} \mathrm{d}u$$

$$\phi(\omega) = \frac{2\omega}{\pi} \int_0^\infty \frac{\ln |G(u)|}{u^2 - \omega^2} \mathrm{d}u \quad (11)$$

It should be noted that complex modulus derived using the physics based principled discussed above automatically satisfy these conditions. However, there can be many other function which would also satisfy these condition. It is possible to determine $G(\omega)$ from experimental measurements (see [24,81]) which satisfy these conditions. In Table 1 we show some functions which have been used in literature. Among various possible viscoelastic models, the Biot's model is considered here.

3. Effective in-plane properties of viscoelastic irregular honeycombs

3.1. Viscoelastic effect on the intrinsic Young's modulus

We consider that each constitutive element of a hexagonal unit with the honeycomb structure is modelled using viscoelastic properties. For simplicity, we use Biot model (see Table 1) with only one term. Frequency dependent complex elastic modulus for an element is expressed as

$$E(\omega) = E_S \left(1 + \epsilon \frac{\mathrm{i}\omega}{\mu + \mathrm{i}\omega} \right) \quad (12)$$

where μ and ϵ are the relaxation parameter and a constant defining the 'strength' of viscosity, respectively. E_s is the intrinsic Young's modulus. The amplitude of this complex elastic modulus is given by

$$|E(\omega)| = E_S \sqrt{\frac{\mu^2 + \omega^2(1 + \epsilon)^2}{\mu^2 + \omega^2}} \quad (13)$$

Table 1
Complex modulus for viscoelastic models in the frequency domain.

Viscoelastic model	Complex modules	Main references
Biot model	$G(\omega) = G_0 + \sum_{k=1}^{n} \frac{a_k i\omega}{i\omega + b_k}$	[8,9]
Fractional derivative	$G(\omega) = \frac{G_0 + G_\infty (i\omega\tau)^\beta}{1 + (i\omega\tau)^\beta}$	[5]
GHM	$G(\omega) = G_0 \left[1 + \sum_k \alpha_k \frac{-\omega^2 + 2i\xi_k \omega_k \omega}{-\omega^2 + 2i\xi_k \omega_k \omega + \omega_k^2} \right]$	[28] and [56]
ADF	$G(\omega) = G_0 \left[1 + \sum_{k=1}^{n} \Delta_k \frac{\omega^2 + i\omega\Omega_k}{\omega^2 + \Omega_k^2} \right]$	[42]
Step-function	$G(\omega) = G_0 \left[1 + \eta \frac{1 - e^{-st_0}}{st_0} \right]$	[1]
Half cosine model	$G(\omega) = G_0 \left[1 + \eta \frac{1 + 2(st_0/\pi)^2 - e^{-st_0}}{1 + 2(st_0/\pi)^2} \right]$	[1]
Gaussian model	$G(\omega) = G_0 \left[1 + \eta\, e^{\omega^2/4\mu} \left\{ 1 - \text{erf}\left(\frac{i\omega}{2\sqrt{\mu}} \right) \right\} \right]$	[2]

The phase (ϕ) of this complex elastic modulus is given by

$$\phi\big(E(\omega)\big) = \tan^{-1}\left(\frac{\epsilon\mu\omega}{\mu^2 + \omega^2(1+\epsilon)} \right) \tag{14}$$

The complex elastic modulus has the following limiting properties, which can be useful in understanding the role of viscoelasticity in the homogenised elastic properties of the honeycomb.

$$|E(\omega)| \to E_S \text{ for } \mu \to \infty \quad \text{and} \quad |E(\omega)| \to E_S(1+\epsilon) \text{ for } \mu \to 0 \quad \forall \omega > 0 \tag{15}$$

$$|E(\omega)| \to E_S \text{ for } \omega \to 0 \quad \text{and} \quad |E(\omega)| \to E_S(1+\epsilon) \text{ for } \omega \to \infty \quad \forall \mu > 0 \tag{16}$$

$$\phi\big(E(\omega)\big) \to 0 \text{ for } \mu \to \infty \quad \text{and} \quad \phi\big(E(\omega)\big) \to 0 \text{ for } \mu \to 0 \quad \forall \omega > 0 \tag{17}$$

$$\phi\big(E(\omega)\big) \to 0 \text{ for } \omega \to 0 \quad \text{and} \quad \phi\big(E(\omega)\big) \to 0 \text{ for } \omega \to \infty \quad \forall \mu > 0 \tag{18}$$

It can be seen that for all these limiting cases, the viscoelastic effects vanish (the phase is zero) and then the material is purely elastic. The cases $\mu \to \infty$ and $\omega \to 0$ correspond to minimum amplitude whiles cases $\mu \to 0$ and $\omega \to \infty$ correspond to maximum amplitude.

3.2. Effective elastic properties of randomly irregular lattices without the effect of viscoelasticity

The elastic moduli with spatially random structural and material attributes have been derived in a previous paper [62] using classical mechanics based principles. The underlying philosophy of the proposed idea is that the entire irregular hexagonal lattice structure consists of several representative unit cell elements (RUCE) at the elementary level as shown in Fig. 1. Each of the RUCEs possess different individual elastic moduli depending on its structural geometry and intrinsic material properties (i.e. $l_1, l_2, l_3, \alpha, \beta, \gamma, E_s$ are different for the RUCEs in spatially irregular lattices; refer to Fig. 1 for the symbols). The effect of irregularity in material and geometric attributes are accounted in the elementary local level first by analysing the RUCEs and then the effect of such irregularity is propagated to the global scale (equivalent in-plane properties of the entire irregular lattice structure). This is achieved by following a multi-scale and multi-stage framework as described in [62]. The closed-form formulae for five in-plane elastic moduli of a single RUCE are derived as a function of their respective material and geometric attributes. Thus the formulae developed for a single RUCE is effectively capable of

expressing the equivalent material properties at local scale. The RUCEs are idealized further in this stage on the basis of the adopted assembling scheme. Subsequently, using the formulae for a single idealized RUCE, the expressions for effective elastic moduli of the entire irregular lattice are derived based on the basic principles of mechanics along with the equilibrium and deformation compatibility conditions following a multi-stage approach. The obtained formulae, which correspond to a generalization of the elastic moduli for perfectly periodic lattices [27], are given below:

$$E_{1eq} = \frac{t^3}{L} \sum_{j=1}^{n} \frac{\sum_{i=1}^{m} \left(l_{1ij} \cos\alpha_{ij} - l_{2ij} \cos\beta_{ij} \right)}{\sum_{i=1}^{m} \frac{l_{1ij}^2 l_{2ij}^2 \left(l_{1ij} + l_{2ij} \right) \left(\cos\alpha_{ij} \sin\beta_{ij} - \sin\alpha_{ij} \cos\beta_{ij} \right)^2}{E_{sij} \left(\left(l_{1ij} \cos\alpha_{ij} - l_{2ij} \cos\beta_{ij} \right)^2 \right)}} \tag{19}$$

$$E_{2eq} = \frac{Lt^3}{\sum_{j=1}^{n} \frac{\sum_{i=1}^{m} \left(l_{1ij} \cos\alpha_{ij} - l_{2ij} \cos\beta_{ij} \right)}{\sum_{i=1}^{m} E_{sij} \left(l_{3ij}^2 \cos^2\gamma_{ij} \left(l_{3ij} + \frac{l_{1ij} l_{2ij}}{l_{1ij} + l_{2ij}} \right) + \frac{l_{1ij}^2 l_{2ij}^2 \left(l_{1ij} + l_{2ij} \right) \cos^2\alpha_{ij} \cos^2\beta_{ij}}{\left(l_{1ij} \cos\alpha_{ij} - l_{2ij} \cos\beta_{ij} \right)^2} \right)^{-1}}} \tag{20}$$

$$v_{12eq} = -\frac{1}{L} \sum_{j=1}^{n} \frac{\sum_{i=1}^{m} \left(l_{1ij} \cos\alpha_{ij} - l_{2ij} \cos\beta_{ij} \right)}{\sum_{i=1}^{m} \frac{\left(\cos\alpha_{ij} \sin\beta_{ij} - \sin\alpha_{ij} \cos\beta_{ij} \right)}{\cos\alpha_{ij} \cos\beta_{ij}}} \tag{21}$$

$$v_{21eq} = -\frac{L}{\sum_{j=1}^{n} \frac{\sum_{i=1}^{m} \left(l_{1ij} \cos\alpha_{ij} - l_{2ij} \cos\beta_{ij} \right)}{\sum_{i=1}^{m} \frac{l_{1ij}^2 l_{2ij}^2 \left(l_{1ij} + l_{2ij} \right) \cos\alpha_{ij} \cos\beta_{ij} \left(\cos\alpha_{ij} \sin\beta_{ij} - \sin\alpha_{ij} \cos\beta_{ij} \right)}{\left(l_{1ij} \cos\alpha_{ij} - l_{2ij} \cos\beta_{ij} \right)^2 \left(l_{3ij}^2 \cos^2\gamma_{ij} \left(l_{3ij} + \frac{l_{1ij} l_{2ij}}{l_{1ij} + l_{2ij}} \right) + \frac{l_{1ij}^2 l_{2ij}^2 \left(l_{1ij} + l_{2ij} \right) \cos^2\alpha_{ij} \cos^2\beta_{ij}}{\left(l_{1ij} \cos\alpha_{ij} - l_{2ij} \cos\beta_{ij} \right)^2} \right)}}} \tag{22}$$

$$G_{12eq} = \frac{Lt^3}{\sum_{j=1}^{n} \frac{\sum_{i=1}^{m} \left(l_{1ij} \cos\alpha_{ij} - l_{2ij} \cos\beta_{ij} \right)}{\sum_{i=1}^{m} E_{sij} \left(l_{3ij}^2 \sin^2\gamma_{ij} \left(l_{3ij} + \frac{l_{1ij} l_{2ij}}{l_{1ij} + l_{2ij}} \right) \right)^{-1}}} \tag{23}$$

Here E_{sij} represents the intrinsic material property of the honeycomb material without viscoelasticity, while the structural dimensions are indicated in Fig. 1(e). The parameter t denotes the thickness of honeycomb cell wall and L is the total length of the lattice. The subscripts i and j ($i = 1, 2, 3, \ldots, m$ and $j = 1, 2, 3, \ldots, n$) are used to indicate location of a RUCE. In the present analysis, the entire irregular lattice is assumed to have m and n number of RUCEs in direction-1 and direction-2, respectively. Thus, to denote a particular parameter, the subscript of ij is used when a RUCE is referred corresponding to a position of ith column and

j^{th} row. From the above expressions, it can be observed that only the two Young's moduli and shear modulus are dependent on the intrinsic material properties of the honeycomb material (E_s), while the two Poisson's ratios are dependent only on the structural geometry of the honeycomb. Thus the two Young's moduli and shear modulus would be influenced by viscoelasticity, but the two Poisson's ratios will remain unaltered. The expressions of Poisson's ratios for the case of viscoelastic material property variation will remain same as Eqs. (21) and (22).

3.3. Effective viscoelastic properties of randomly irregular lattices

Based on the elastic-viscoelastic correspondence principle [12] and the discussion furnished in Section 3.1, the expressions for two Young's moduli and shear modulus accounting the viscoelastic effect can be obtained easily in the frequency domain by replacing Young's modulus E_{sij} in Eqs. (21) and (22) by the frequency dependent Young's modulus $E_{sij}\left(1 + \epsilon_{ij}\dfrac{i\omega}{\mu_{ij} + i\omega}\right)$. We then obtain

$$E_{1v}(\omega) = \frac{t^3}{L}\sum_{j=1}^{n}\frac{\sum_{i=1}^{m}\left(l_{1ij}\cos\alpha_{ij} - l_{2ij}\cos\beta_{ij}\right)}{\sum_{i=1}^{m}\dfrac{l_{1ij}^2 l_{2ij}^2\left(l_{1ij} + l_{2ij}\right)\left(\cos\alpha_{ij}\sin\beta_{ij} - \sin\alpha_{ij}\cos\beta_{ij}\right)^2}{E_{sij}\left(1 + \epsilon_{ij}\dfrac{i\omega}{\mu_{ij} + i\omega}\right)\left(\left(l_{1ij}\cos\alpha_{ij} - l_{2ij}\cos\beta_{ij}\right)^2\right)}}$$
(24)

$$E_{2v}(\omega) = \frac{Lt^3}{\sum_{j=1}^{n}\dfrac{\sum_{i=1}^{m}\left(l_{1ij}\cos\alpha_{ij} - l_{2ij}\cos\beta_{ij}\right)}{\sum_{i=1}^{m}E_{sij}\left(1 + \epsilon_{ij}\dfrac{i\omega}{\mu_{ij} + i\omega}\right)\left(l_{3ij}^2\cos^2\gamma_{ij}\left(l_{3ij} + \dfrac{l_{1ij}l_{2ij}}{l_{1ij} + l_{2ij}}\right) + \dfrac{l_{1ij}^2 l_{2ij}^2\left(l_{1ij} + l_{2ij}\right)\cos^2\alpha_{ij}\cos^2\beta_{ij}}{\left(l_{1ij}\cos\alpha_{ij} - l_{2ij}\cos\beta_{ij}\right)^2}\right)^{-1}}}$$
(25)

$$G_{12v}(\omega) = \frac{Lt^3}{\sum_{j=1}^{n}\dfrac{\sum_{i=1}^{m}\left(l_{1ij}\cos\alpha_{ij} - l_{2ij}\cos\beta_{ij}\right)}{\sum_{i=1}^{m}E_{sij}\left(1 + \epsilon_{ij}\dfrac{i\omega}{\mu_{ij} + i\omega}\right)\left(l_{3ij}^2\sin^2\gamma_{ij}\left(l_{3ij} + \dfrac{l_{1ij}l_{2ij}}{l_{1ij} + l_{2ij}}\right)\right)^{-1}}}$$
(26)

The above expressions allow us to consider spatially varying structural attributes and viscoelastic material properties. It can be noted that the above expressions provide complex values of the viscoelastic moduli, from which the respective amplitudes and phase angles can be obtained numerically. The effective elastic moduli of irregular viscoelastic lattices with spatially correlated material and structural attributes are obtained by integrating the above closed-form expressions (as furnished in Sections 3.2 and 3.3) and the Karhunen–Loève expansion, as described in Section 4.

3.4. Remark 1: effective viscoelastic properties of hexagonal lattices with only spatial variation of material properties

According to the notations used for a regular honeycomb by Gibson and Ashby (1999) (as shown in Fig. 1(d)), the notations of the present paper for honeycombs without any structural irregularity can be expressed as: $L = n(h + l\sin\theta)$; $l_{1ij} = l_{2ij} = l_{3ij} = l$; $\alpha_{ij} = \theta$; $\beta_{ij} = 180° - \theta$; $\gamma_{ij} = 90°$, for all i and j. Using these transformations in case of the spatial variation of only material properties, the structural parameter in

Eqs. (24)–(26) can be put out of the sums and the closed-form formulae for compound variation of material and geometric properties are simplified as

$$E_{1v} = \kappa_1\left(\frac{t}{l}\right)^3\frac{\cos\theta}{\left(\frac{h}{l} + \sin\theta\right)\sin^2\theta}$$
(27)

$$E_{2v} = \kappa_2\left(\frac{t}{l}\right)^3\frac{\left(\frac{h}{l} + \sin\theta\right)}{\cos^3\theta}$$
(28)

$$\text{and}\quad G_{12v} = \kappa_2\left(\frac{t}{l}\right)^3\frac{\left(\frac{h}{l} + \sin\theta\right)}{\left(\frac{h}{l}\right)^2\left(1 + 2\frac{h}{l}\right)\cos\theta}$$
(29)

The multiplication factors κ_1 and κ_2 arising due to the consideration of spatially random variation of intrinsic material properties can be expressed as

$$\kappa_1 = \frac{m}{n}\sum_{j=1}^{n}\frac{1}{\sum_{i=1}^{m}\dfrac{1}{E_{sij}\left(1 + \epsilon_{ij}\dfrac{i\omega}{\mu_{ij} + i\omega}\right)}}$$
(30)

$$\text{and}\quad \kappa_2 = \frac{n}{m}\frac{1}{\sum_{j=1}^{n}\dfrac{1}{\sum_{i=1}^{m}E_{sij}\left(1 + \epsilon_{ij}\dfrac{i\omega}{\mu_{ij} + i\omega}\right)}}$$
(31)

The expressions of κ_1 and κ_2 are complex in nature and include the viscoelastic material properties. Thus the effective elastic moduli presented in Eqs. (27)–(29) are also complex valued and dependent on the spatially random variation of intrinsic material property and the viscoelastic parameters. The amplitude and phase angle of the three complex valued in-plane elastic moduli can be obtained numerically. In the special case when $\omega \to 0$ and there is no spatial variabilities in the material properties of the lattice, all viscoelastic material properties become identical (i.e. $E_{sij} = E_s$, $\mu_{ij} = \mu$ and $\epsilon_{ij} = \epsilon$ for $i = 1, 2, 3, \ldots, m$ and $j = 1, 2, 3, \ldots, n$) and subsequently the amplitude of κ_1 and κ_2 becomes exactly E_s. This confirms that the expressions in Eqs. (30) and (31) give the necessary generalisations of the classical expressions of Gibson and Ashby (1999) through Eqs. (27)–(29).

3.5. Remark 2: effective viscoelastic properties of hexagonal lattices with only structural irregularity

In case of only spatially random variation of structural geometry but constant viscoelastic material properties (i.e. $E_{sij} = E_s$, $\mu_{ij} = \mu$ and $\epsilon_{ij} = \epsilon$ for $i = 1, 2, 3, \ldots, m$ and $j = 1, 2, 3, \ldots, n$) the Eqs. (24)–(26) lead to

$$E_{1v} = E_S\left(1 + \epsilon\frac{i\omega}{\mu + i\omega}\right)\zeta_1$$
(32)

$$E_{2v} = E_S\left(1 + \epsilon\frac{i\omega}{\mu + i\omega}\right)\zeta_2$$
(33)

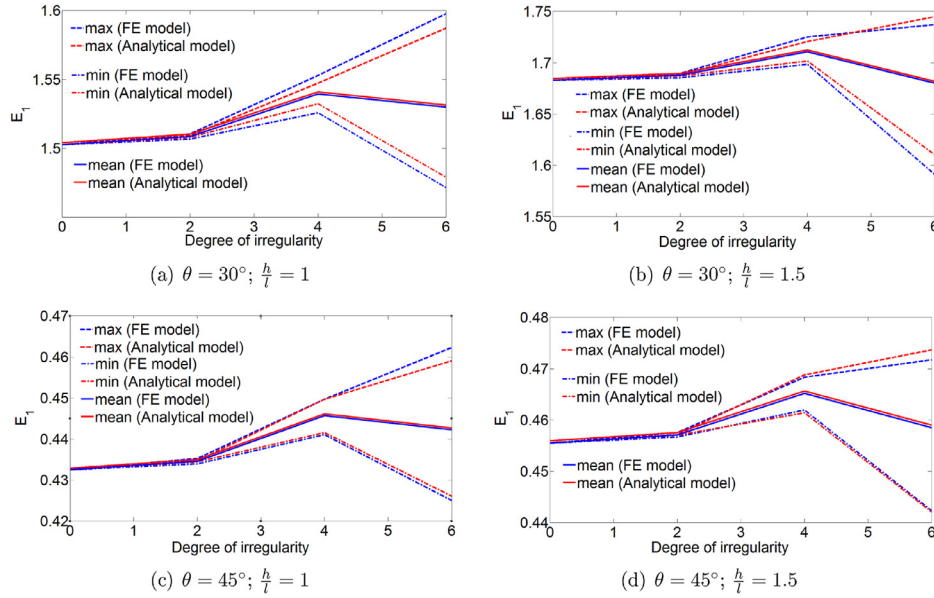$$G_{12v} = E_S\left(1 + \epsilon\frac{i\omega}{\mu + i\omega}\right)\zeta_3$$
(34)

Fig. 3. Effective Young's modulus (E_1) of irregular lattices with different structural configurations considering correlated attributes.
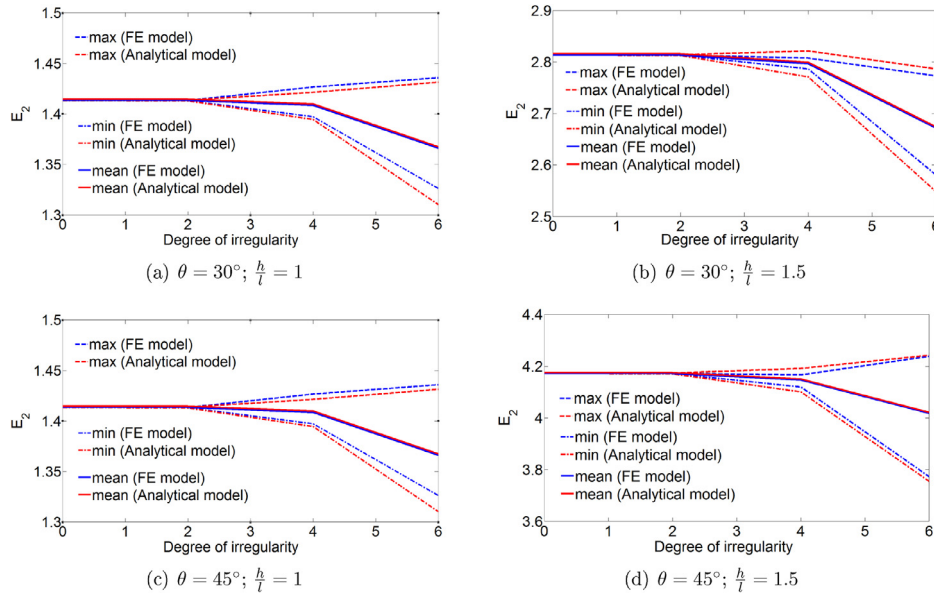

Fig. 4. Effective Young's modulus (E_2) of irregular lattices with different structural configurations considering correlated attributes.

where ζ_i ($i = 1, 2, 3$) are the factors concerning spatially random variation of structural geometry. These factors can be expressed as

$$\zeta_1 = \frac{t^3}{L} \sum_{j=1}^{n} \frac{\sum_{i=1}^{m} \left(l_{1ij} \cos \alpha_{ij} - l_{2ij} \cos \beta_{ij}\right)}{\sum_{i=1}^{m} \frac{l_{1ij}^2 l_{2ij}^2 \left(l_{1ij} + l_{2ij}\right)\left(\cos \alpha_{ij} \sin \beta_{ij} - \sin \alpha_{ij} \cos \beta_{ij}\right)^2}{\left(l_{1ij} \cos \alpha_{ij} - l_{2ij} \cos \beta_{ij}\right)^2}} \tag{35}$$

$$\zeta_2 = \frac{Lt^3}{\sum_{j=1}^{n} \frac{\sum_{i=1}^{m} \left(l_{1ij} \cos \alpha_{ij} - l_{2ij} \cos \beta_{ij}\right)}{\sum_{i=1}^{m} \left(l_{3ij}^2 \cos^2 \gamma_{ij} \left(l_{3ij} + \frac{l_{1ij} l_{2ij}}{l_{1ij} + l_{2ij}}\right) + \frac{l_{1ij}^2 l_{2ij}^2 \left(l_{1ij} + l_{2ij}\right) \cos^2 \alpha_{ij} \cos^2 \beta_{ij}}{\left(l_{1ij} \cos \alpha_{ij} - l_{2ij} \cos \beta_{ij}\right)^2}\right)^{-1}}} \tag{36}$$

$$\zeta_3 = \frac{Lt^3}{\sum_{j=1}^{n} \frac{\sum_{i=1}^{m} \left(l_{1ij} \cos \alpha_{ij} - l_{2ij} \cos \beta_{ij}\right)}{\sum_{i=1}^{m} \left(l_{3ij}^2 \sin^2 \gamma_{ij} \left(l_{3ij} + \frac{l_{1ij} l_{2ij}}{l_{1ij} + l_{2ij}}\right)\right)^{-1}}} \tag{37}$$

The amplitude of the three viscoelastic moduli for the case of only spatially random variation of structural geometry can be expressed as

$$|E_{1v}| = E_s \zeta_1 \sqrt{\frac{\mu^2 + \omega^2 (1 + \epsilon)^2}{\mu^2 + \omega^2}} \tag{38}$$

$$|E_{2v}| = E_s \zeta_2 \sqrt{\frac{\mu^2 + \omega^2 (1 + \epsilon)^2}{\mu^2 + \omega^2}} \tag{39}$$

$$|G_{12v}| = E_s \zeta_3 \sqrt{\frac{\mu^2 + \omega^2 (1 + \epsilon)^2}{\mu^2 + \omega^2}} \tag{40}$$
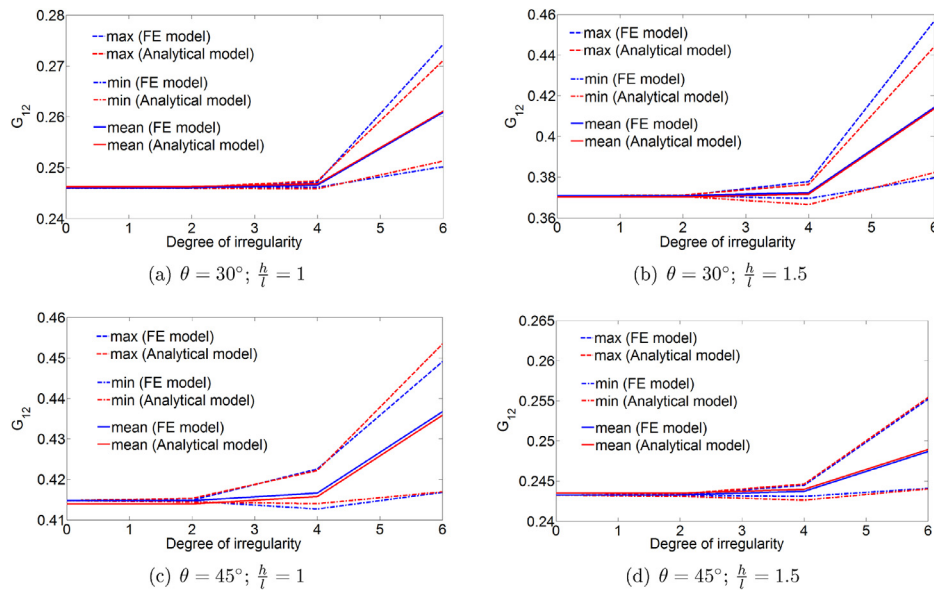
Fig. 5. Effective shear modulus (G_{12}) of irregular lattices with different structural configurations considering correlated attributes.
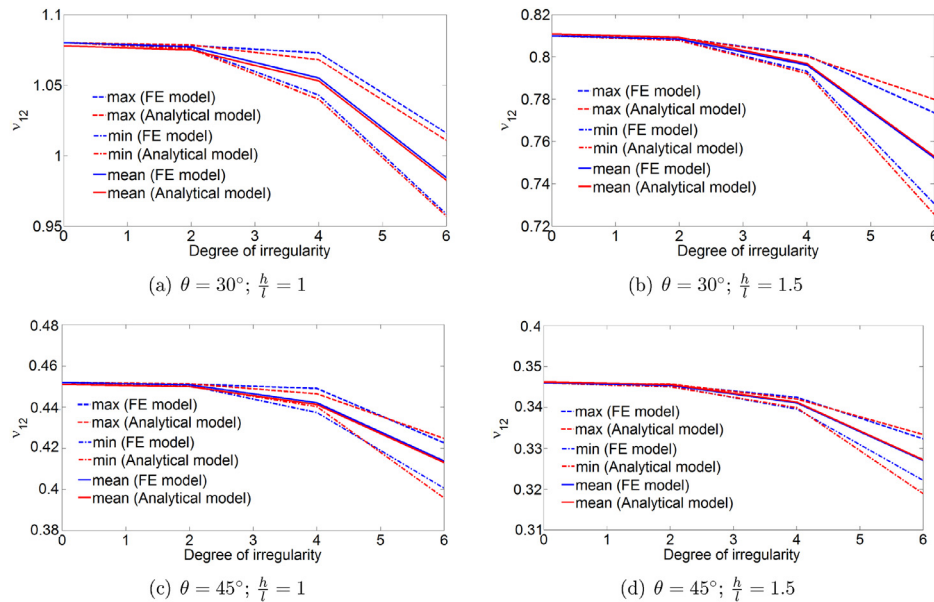

Fig. 6. Effective Poisson's ratio (ν_{12}) of irregular lattices with different structural configurations considering correlated attributes.

The phase (ϕ) of the three complex elastic moduli corresponding to the case of only spatially random variation of structural geometry are given by

$$\phi(E_{1v}) = \phi(E_{2v}) = \phi(G_{12v}) = \tan^{-1}\left(\frac{\epsilon\mu\omega}{\mu^2 + \omega^2(1+\epsilon)}\right) \quad (41)$$

From the above expression it is interesting to notice that the phase angle in case of regular lattice configurations are not dependent on the structural geometry and they are same for the three in-plane elastic moduli. This result is expected since, for this case, the viscoelasticity parameters are the same in all the cells of the lattice, the global time delay induced by the viscoelastic effects of the material is the same compared to the ones related to each cell. The amplitude of the elastic moduli obtained based on the above expressions converge to the closed-form equation provided by [27] in the limiting case of $\omega \to 0$ and regular structural configuration (i.e. $L = n(h + l\sin\theta)$; $l_{1ij} = l_{2ij} = l_{3ij} = l$; $\alpha_{ij} = \theta$; $\beta_{ij} = 180° - \theta$; $\gamma_{ij} = 90°$, for all i and j). For the limiting cases $\mu \to 0$, $\mu \to \infty$, $\omega \to 0$, $\omega \to \infty$, Eqs. (38)–(41) for the viscosity dependent

in-plane elastic properties simplify as

$$|E_{1v}| \to E_S\zeta_1 \text{ for } \mu \to \infty \quad \text{and} \quad |E_{1v}| \to E_S(1+\epsilon)\zeta_1 \text{ for } \mu \to 0 \quad \forall \omega > 0 \quad (42)$$

$$|E_{1v}| \to E_S\zeta_1 \text{ for } \omega \to 0 \quad \text{and} \quad |E_{1v}| \to E_S(1+\epsilon)\zeta_1 \text{ for } \omega \to \infty \quad \forall \mu > 0 \quad (43)$$

$$|E_{2v}| \to E_S\zeta_2 \text{ for } \mu \to \infty \quad \text{and} \quad |E_{2v}| \to E_S(1+\epsilon)\zeta_2 \text{ for } \mu \to 0 \quad \forall \omega > 0 \quad (44)$$

$$|E_{2v}| \to E_S\zeta_2 \text{ for } \omega \to 0 \quad \text{and} \quad |E_{2v}| \to E_S(1+\epsilon)\zeta_2 \text{ for } \omega \to \infty \quad \forall \mu > 0 \quad (45)$$

$$|G_{12v}| \to E_S\zeta_3 \text{ for } \mu \to \infty \quad \text{and} \quad |G_{12v}| \to E_S(1+\epsilon)\zeta_3 \text{ for } \mu \to 0 \quad \forall \omega > 0 \quad (46)$$
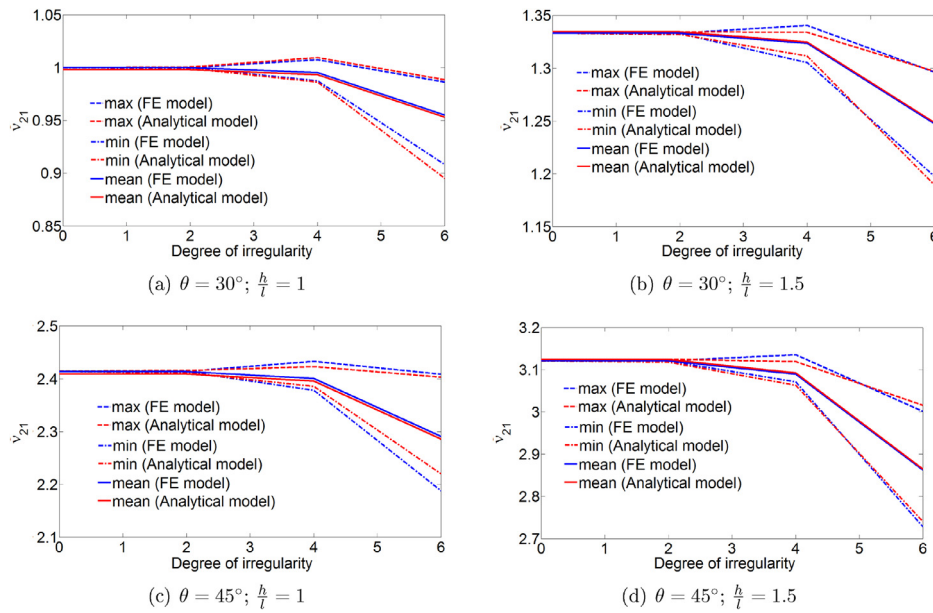
Fig. 7. Effective Poisson's ratio (ν_{21}) of irregular lattices with different structural configurations considering correlated attributes.
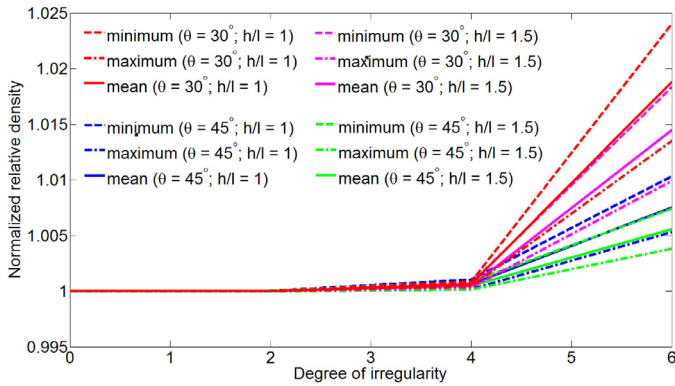

Fig. 8. Effective normalized relative density (normalized with respect to the corresponding relative density of regular structural configurations) of irregular lattices with different structural configurations considering correlated attributes.

$$|G_{12v}| \to E_S \zeta_3 \text{ for } \omega \to 0 \quad \text{and} \quad |G_{12v}| \to E_S(1+\epsilon)\zeta_3 \text{ for } \omega \to \infty \quad \forall \mu > 0 \tag{47}$$

$$\phi(E_{1v}), \quad \phi(E_{2v}), \quad \phi(G_{12v}) \to 0 \text{ for } \mu \to \infty \tag{48}$$

$$\text{and} \quad \phi(E_{1v}), \quad \phi(E_{2v}), \quad \phi(G_{12v}) \to 0 \text{ for } \mu \to 0 \quad \forall \omega > 0 \tag{49}$$

$$\phi(E_{1v}), \quad \phi(E_{2v}), \quad \phi(G_{12v}) \to 0 \text{ for } \omega \to 0 \tag{50}$$

$$\text{and} \quad \phi(E_{1v}), \quad \phi(E_{2v}), \quad \phi(G_{12v}) \to 0 \text{ for } \omega \to \infty \quad \forall \mu > 0 \tag{51}$$

3.6. Remark 3: effective viscoelastic properties of regular hexagonal lattices

The closed-form expressions for all the in-plane elastic moduli (without the viscoelastic effect) of irregular lattices in Eqs. (19)–(23) can be reduced to the formulae provided by [27] in the special case of uniform honeycombs. According to the notations used for a regular honeycomb by [27] as shown in Fig. 1(d), the geometric notations of the

present paper for regular lattices can be expressed as: $L = n(h + l \sin\theta)$; $l_{1ij} = l_{2ij} = l_{3ij} = l$; $\alpha_{ij} = \theta$; $\beta_{ij} = 180° - \theta$; $\gamma_{ij} = 90°$, for all i and j. Using these transformations in Eqs. (19)–(23), the expressions of in-plane elastic moduli for regular hexagonal lattices (without the viscoelastic effect) can be obtained.

The in-plane Poisson's ratios are not dependent on the viscoelastic properties, as discussed in the preceding subsection. For regular honeycombs with viscoelastic effect, the geometrical transformations described in the preceding paragraph are applicable along with $E_{sij} = E_s$, $\mu_{ij} = \mu$ and $\epsilon_{ij} = \epsilon$ for $i = 1, 2, 3, \ldots, m$ and $j = 1, 2, 3, \ldots, n$. Thus, based on Eqs. (24)–(26), the in-plane Young's moduli and shear modulus (viscosity dependent in-plane elastic properties) can be expressed as

$$E_{1v} = E_s \left(1 + \epsilon \frac{i\omega}{\mu + i\omega}\right)\left(\frac{t}{l}\right)^3 \frac{\cos\theta}{\left(\frac{h}{l} + \sin\theta\right)\sin^2\theta} \tag{52}$$

$$E_{2v} = E_s \left(1 + \epsilon \frac{i\omega}{\mu + i\omega}\right)\left(\frac{t}{l}\right)^3 \frac{\left(\frac{h}{l} + \sin\theta\right)}{\cos^3\theta} \tag{53}$$

$$G_{12v} = E_s \left(1 + \epsilon \frac{i\omega}{\mu + i\omega}\right)\left(\frac{t}{l}\right)^3 \frac{\left(\frac{h}{l} + \sin\theta\right)}{\left(\frac{h}{l}\right)^2\left(1 + 2\frac{h}{l}\right)\cos\theta} \tag{54}$$

The amplitude of the three viscoelastic moduli are given by

$$|E_{1v}| = E_s \sqrt{\frac{\mu^2 + \omega^2(1+\epsilon)^2}{\mu^2 + \omega^2}}\left(\frac{t}{l}\right)^3 \frac{\cos\theta}{\left(\frac{h}{l} + \sin\theta\right)\sin^2\theta} \tag{55}$$

$$|E_{2v}| = E_s \sqrt{\frac{\mu^2 + \omega^2(1+\epsilon)^2}{\mu^2 + \omega^2}}\left(\frac{t}{l}\right)^3 \frac{\left(\frac{h}{l} + \sin\theta\right)}{\cos^3\theta} \tag{56}$$

$$|G_{12v}| = E_s \sqrt{\frac{\mu^2 + \omega^2(1+\epsilon)^2}{\mu^2 + \omega^2}}\left(\frac{t}{l}\right)^3 \frac{\left(\frac{h}{l} + \sin\theta\right)}{\left(\frac{h}{l}\right)^2(1 + 2\frac{h}{l})\cos\theta} \tag{57}$$

The phase (ϕ) of the three complex elastic moduli corresponding to regular configuration are given by

$$\phi(E_{1v}) = \phi(E_{2v}) = \phi(G_{12v}) = \tan^{-1}\left(\frac{\epsilon\mu\omega}{\mu^2 + \omega^2(1+\epsilon)}\right) \tag{58}$$

From the above expression, as expected, again the phase angle in case of regular lattice configurations are not dependent on the structural geometry and they are same for the three in-plane elastic moduli. It can also
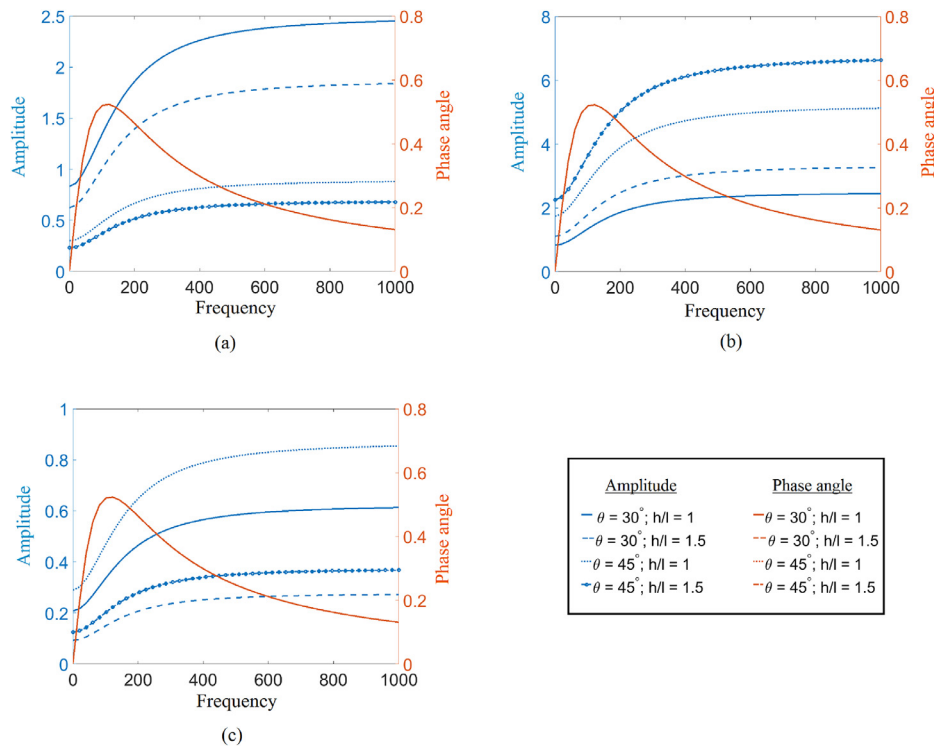
Fig. 9. (a) Effect of viscoelasticity on the magnitude and phase angle of E_1 for regular hexagonal lattices (b) Effect of viscoelasticity on the magnitude and phase angle of E_2 for regular hexagonal lattices (c) Effect of viscoelasticity on the magnitude and phase angle of G_{12} for regular hexagonal lattices.
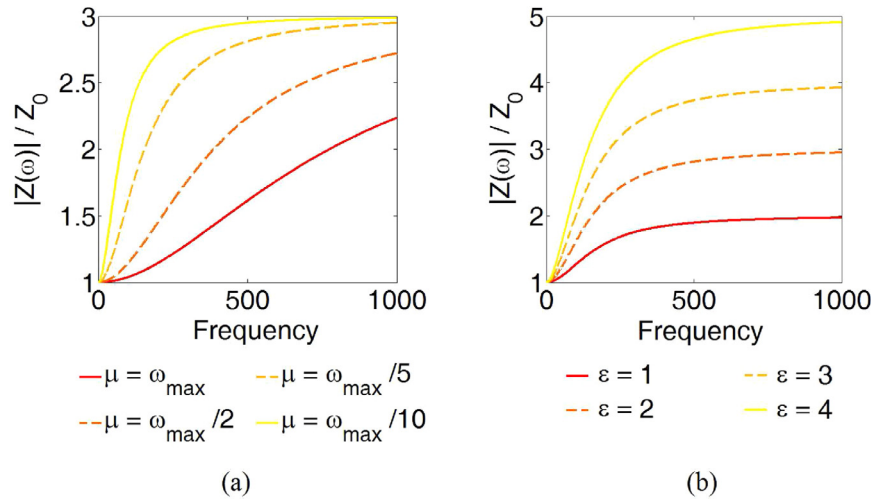

Fig. 10. (a) Effect of variation of μ on the viscoelastic modulus of regular hexagonal lattices (considering a constant value of $\epsilon = 2$) (b) Effect of variation of ϵ on the viscoelastic modulus of regular hexagonal lattices (considering a constant value of $\mu = \omega_{max}/5$). Here Z represents the viscoelastic moduli (i.e. E_1, E_2 and G_{12}) and Z_0 is the corresponding elastic modulus value for $\omega = 0$.

be noticed that the expressions of phase angle are identical to the special case considered in Section 3.5. The amplitude of the elastic moduli obtained based on the above expressions converge to the closed-form equation provided by Gibson and Ashby [27] in the limiting case of $\omega \to 0$. Again, for the limiting cases $\mu \to 0$, $\mu \to \infty$, $\omega \to 0$, $\omega \to \infty$, the viscosity dependent in-plane elastic properties simplify as

$$|E_{1v}| \to E_S\left(\frac{t}{l}\right)^3 \frac{\cos\theta}{\left(\frac{h}{l} + \sin\theta\right)\sin^2\theta} \quad \text{for } \mu \to \infty \tag{59}$$

$$\text{and} \quad |E_{1v}| \to E_S(1+\epsilon)\left(\frac{t}{l}\right)^3 \frac{\cos\theta}{\left(\frac{h}{l} + \sin\theta\right)\sin^2\theta} \quad \text{for } \mu \to 0 \quad \forall \omega > 0 \tag{60}$$

$$|E_{1v}| \to E_S\left(\frac{t}{l}\right)^3 \frac{\cos\theta}{\left(\frac{h}{l} + \sin\theta\right)\sin^2\theta} \quad \text{for } \omega \to 0 \tag{61}$$

$$\text{and} \quad |E_{1v}| \to E_S(1+\epsilon)\left(\frac{t}{l}\right)^3 \frac{\cos\theta}{\left(\frac{h}{l} + \sin\theta\right)\sin^2\theta} \quad \text{for } \omega \to \infty \quad \forall \mu > 0 \tag{62}$$

$$|E_{2v}| \to E_S\left(\frac{t}{l}\right)^3 \frac{\left(\frac{h}{l} + \sin\theta\right)}{\cos^3\theta} \quad \text{for } \mu \to \infty \tag{63}$$

$$\text{and} \quad |E_{2v}| \to E_S(1+\epsilon)\left(\frac{t}{l}\right)^3 \frac{\left(\frac{h}{l} + \sin\theta\right)}{\cos^3\theta} \quad \text{for } \mu \to 0 \quad \forall \omega > 0 \tag{64}$$

Fig. 11. (a) Effect of variation of μ on the phase angle of regular hexagonal lattices (considering a constant value of $\mu = \omega_{max}/5$) (b) Effect of variation of ϵ on the phase angle of regular hexagonal lattices (considering a constant value of $\mu = \omega_{max}/5$). Here Z represents the complex viscoelastic moduli (i.e. E_1, E_2 and G_{12})
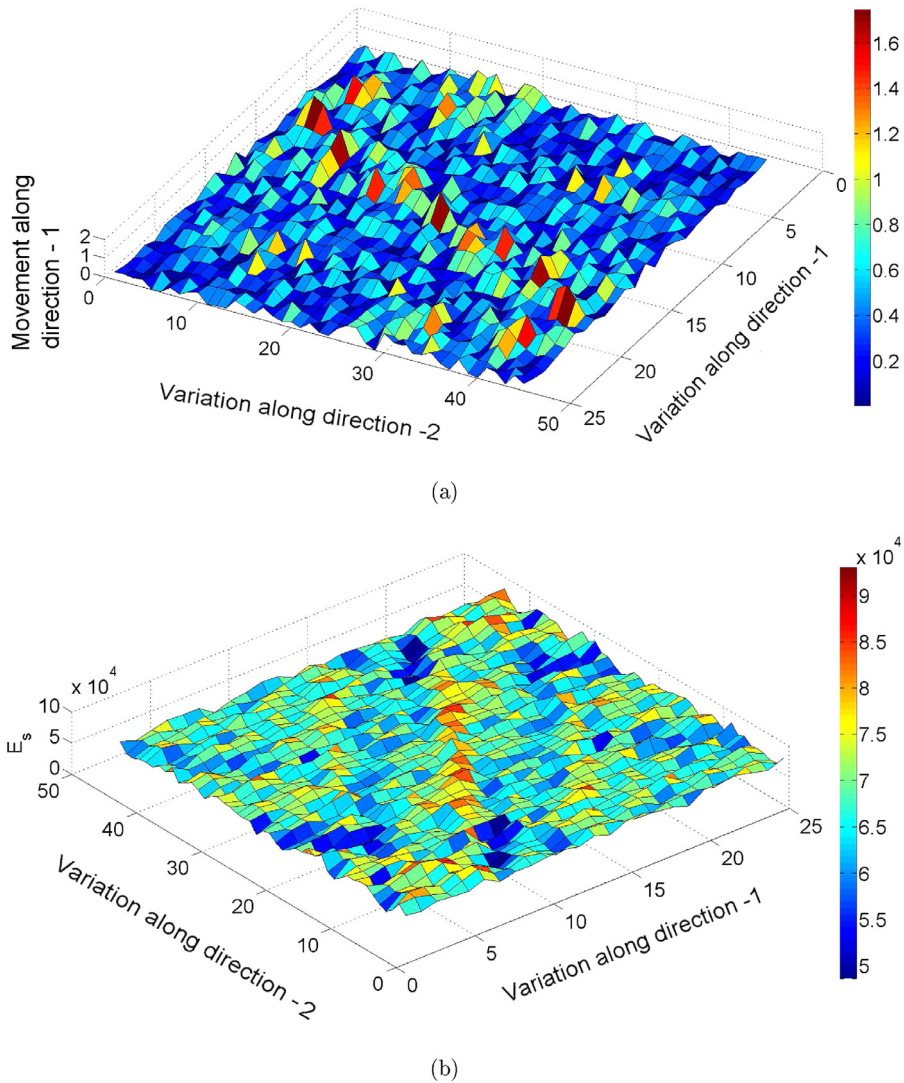
Fig. 12. Typical representation of random fields for a particular realization considered in the analysis for (a) movement of the top vertices of a tessellating hexagonal unit cell with respect to the corresponding deterministic locations ($r = 6$) (b) intrinsic elastic modulus (E_s) with $\Delta_m = 0.002$.
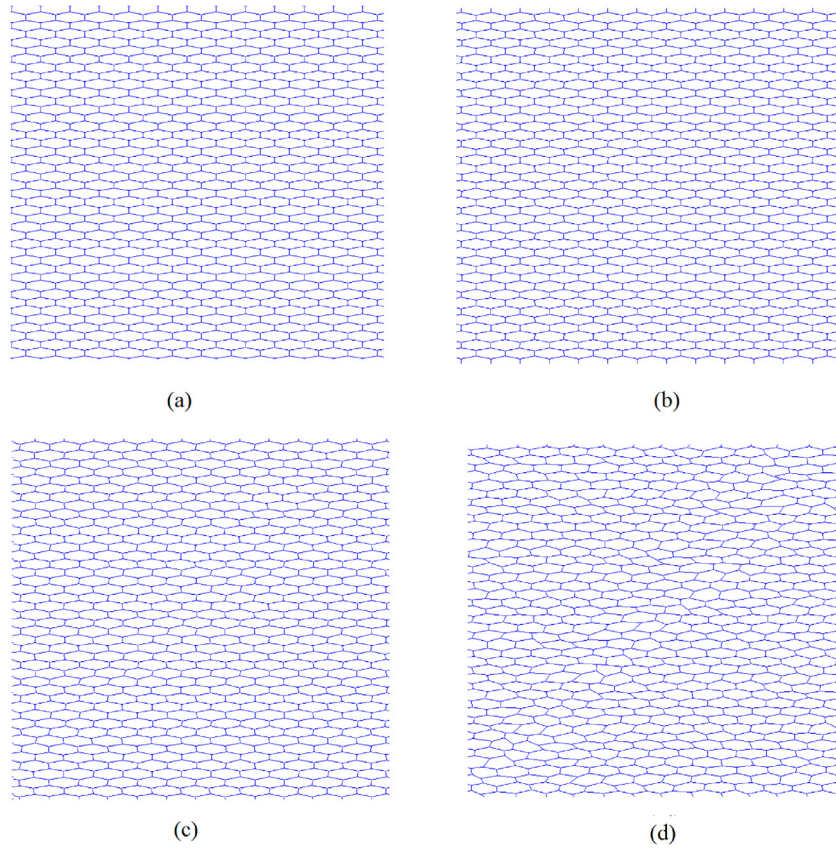
Fig. 13. Structural configurations for a single random realization of an irregular hexagonal lattice considering deterministic cell angle $\theta = 30°$ and $h/l = 1$: (a) $r = 0$ (b) $r = 2$ (c) $r = 4$ (d) $r = 6$.
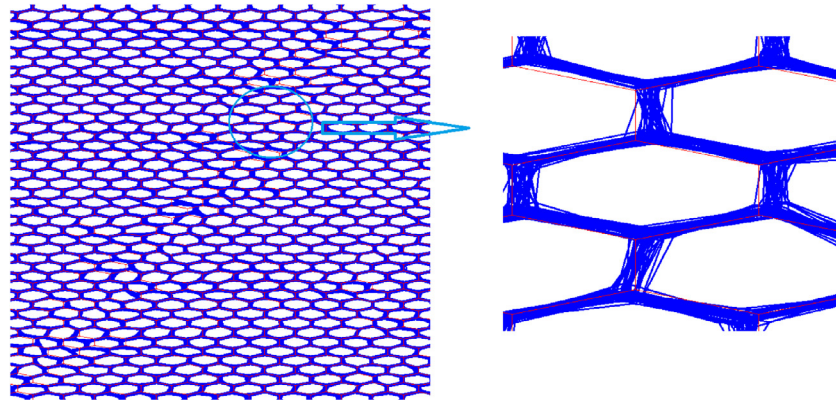
Fig. 14. Simulation bound of the structural configuration of an irregular hexagonal lattice for multiple random realizations considering $\theta = 30°$, $h/l = 1$ and $r = 6$. The regular configuration is presented using red colour. (For interpretation of the references to color in this figure legend, the reader is referred to the web version of this article.)

$$|E_{2v}| \rightarrow E_S \left(\frac{t}{l}\right)^3 \frac{\left(\frac{h}{l} + \sin\theta\right)}{\cos^3\theta} \text{ for } \omega \rightarrow 0 \tag{65}$$

$$\text{and} \quad |E_{2v}| \rightarrow E_S(1+\epsilon)\left(\frac{t}{l}\right)^3 \frac{\left(\frac{h}{l} + \sin\theta\right)}{\cos^3\theta} \text{ for } \omega \rightarrow \infty \quad \forall \mu > 0 \tag{66}$$
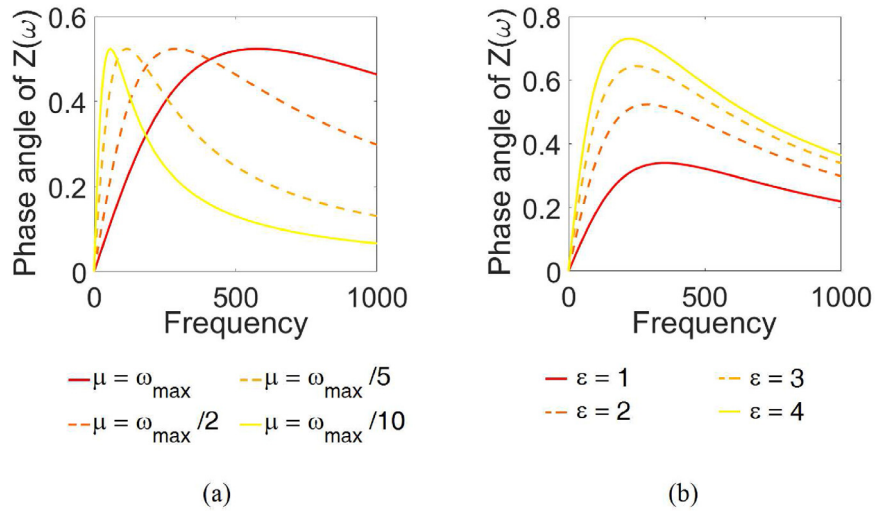
$$|G_{12v}| \rightarrow E_S \left(\frac{t}{l}\right)^3 \frac{\left(\frac{h}{l} + \sin\theta\right)}{\left(\frac{h}{l}\right)^2 (1 + 2\frac{h}{l})\cos\theta} \text{ for } \mu \rightarrow \infty \tag{67}$$

$$\text{and} \quad |G_{12v}| \rightarrow E_S(1+\epsilon)\left(\frac{t}{l}\right)^3 \frac{\left(\frac{h}{l} + \sin\theta\right)}{\left(\frac{h}{l}\right)^2 (1 + 2\frac{h}{l})\cos\theta} \text{ for } \mu \rightarrow 0 \quad \forall \omega > 0 \tag{68}$$

$$|G_{12v}| \rightarrow E_S \left(\frac{t}{l}\right)^3 \frac{\left(\frac{h}{l} + \sin\theta\right)}{\left(\frac{h}{l}\right)^2 (1 + 2\frac{h}{l})\cos\theta} \text{ for } \omega \rightarrow 0 \tag{69}$$

$$\text{and} \quad |G_{12v}| \rightarrow E_S(1+\epsilon)\left(\frac{t}{l}\right)^3 \frac{\left(\frac{h}{l} + \sin\theta\right)}{\left(\frac{h}{l}\right)^2 (1 + 2\frac{h}{l})\cos\theta} \text{ for } \omega \rightarrow \infty \quad \forall \mu > 0 \tag{70}$$

$$\phi(E_{1v}), \quad \phi(E_{2v}), \quad \phi(G_{12v}) \rightarrow 0 \text{ for } \mu \rightarrow \infty \tag{71}$$

$$\text{and} \quad \phi(E_{1v}), \quad \phi(E_{2v}), \quad \phi(G_{12v}) \rightarrow 0 \text{ for } \mu \rightarrow 0 \quad \forall \omega > 0 \tag{72}$$

$$\phi(E_{1v}), \quad \phi(E_{2v}), \quad \phi(G_{12v}) \rightarrow 0 \text{ for } \omega \rightarrow 0 \tag{73}$$

Fig. 15. Effect of viscoelasticity on Young's modulus E_1 corresponding to randomly correlated inhomogeneous lattices having spatial structural irregularity. Frequency dependent amplitudes and phase angles are presented for various cellular configurations considering two different degree of structural irregularity ($r = 3$ and $r = 6$).

and $\quad \phi(E_{1v}), \quad \phi(E_{2v}), \quad \phi(G_{12v}) \to 0$ for $\omega \to \infty \quad \forall \mu > 0 \qquad$ (74)

In the case of regular uniform honeycombs with $\theta = 30°$, we have

$$E_{1v} = E_{2v} = 2.3 E_S \left(1 + \epsilon \frac{i\omega}{\mu + i\omega}\right) \left(\frac{t}{l}\right)^3 \qquad (75)$$

Similarly, in the case of shear modulus for regular uniform honeycombs ($\theta = 30°$)

$$G_{12v} = 0.57 E_S \left(1 + \epsilon \frac{i\omega}{\mu + i\omega}\right) \left(\frac{t}{l}\right)^3 \qquad (76)$$

The amplitude of the three viscoelastic moduli for regular uniform honeycomb are given by

$$|E_{1v}| = |E_{2v}| = 2.3 E_s \sqrt{\frac{\mu^2 + \omega^2(1 + \epsilon)^2}{\mu^2 + \omega^2}} \left(\frac{t}{l}\right)^3 \qquad (77)$$

$$|G_{12v}| = 0.57 E_s \sqrt{\frac{\mu^2 + \omega^2(1 + \epsilon)^2}{\mu^2 + \omega^2}} \left(\frac{t}{l}\right)^3 \qquad (78)$$

The phase (ϕ) of the three complex elastic moduli corresponding to regular configuration are given by

$$\phi(E_{1v}) = \phi(E_{2v}) = \phi(G_{12v}) = \tan^{-1}\left(\frac{\epsilon\mu\omega}{\mu^2 + \omega^2(1 + \epsilon)}\right) \qquad (79)$$

Limiting values for the amplitude and phase angle of the three viscoelastic moduli for regular uniform honeycomb can be obtained by substituting $\theta = 30°$ in Eqs. (60)–(74).

Regular viscoelastic honeycombs satisfy the reciprocal theorem

$$E_{2v}v_{12v} = E_{1v}v_{21v} = E_S \left(1 + \epsilon \frac{i\omega}{\mu + i\omega}\right) \left(\frac{t}{l}\right)^3 \frac{1}{\sin\theta\cos\theta} \qquad (80)$$

It is noteworthy that for regular uniform honeycombs, the Poisson's ratios become unity (i.e. $v_{12} = v_{21} = 1$) and the regular uniform honeycombs with viscoelastic properties correctly obey the relation $G = E/2(1 + v)$, where E, G and v represent Young's modulus, shear modulus and Poisson's ratio of isotropic viscoelastic solids respectively.
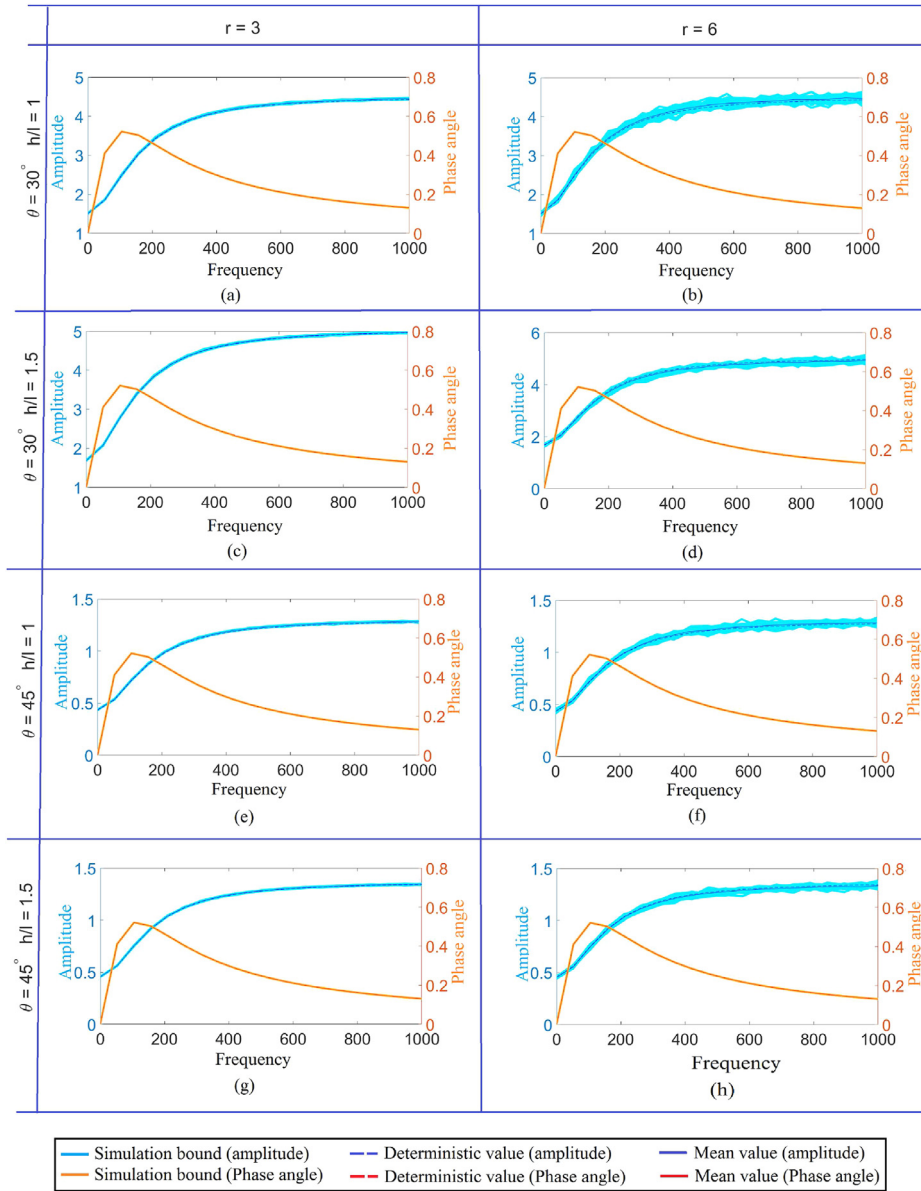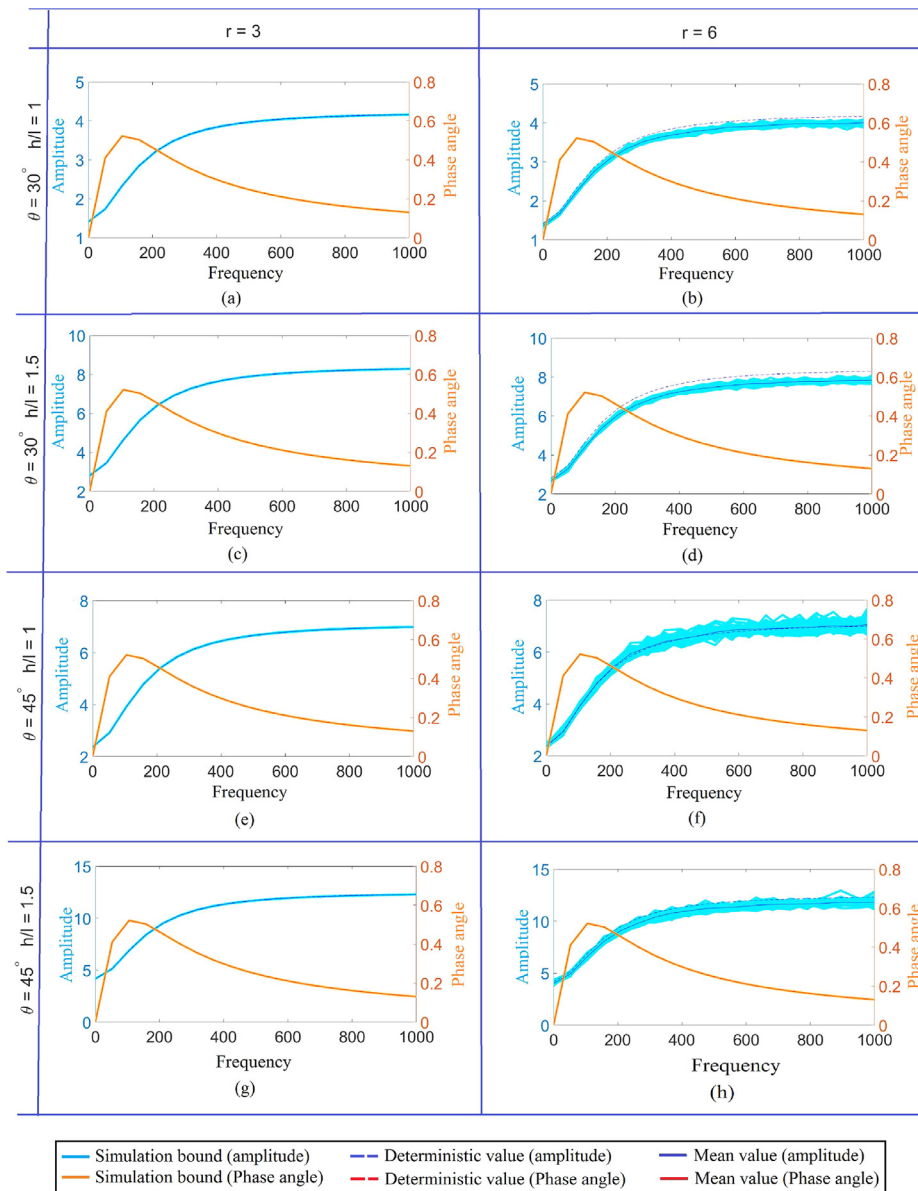
Fig. 16. Effect of viscoelasticity on Young's modulus E_2 corresponding to randomly correlated inhomogeneous lattices having spatial structural irregularity. Frequency dependent amplitudes and phase angles are presented for various cellular configurations considering two different degree of structural irregularity ($r = 3$ and $r = 6$).

4. Effective viscoelastic properties of irregular lattices with correlated structural and material attributes based on Karhunen–Loève expansion

Let's introduce the probability space $(\Theta, \mathcal{F}, \mathcal{P})$, where Θ, $\mathcal{F}$ and $\mathcal{P}$ are the classical sample space, $\sigma-$algebra and probability measure respectively. Let $\mathcal{H}(\mathbf{x}, \theta)$ be a random fields defined on $(\Theta, \mathcal{F}, \mathcal{P})$, where $\theta \in \Theta$ is an outcome and $\mathbf{x}$ is the spatial coordinates. In this section, $\mathcal{H}(\mathbf{x}, \theta)$ is a general notation for a random field and can represent the random structural parameters (coordinates of the nodes of a lattice) or the random material properties parameters (Young's moduli and viscoelastic parameters). There are a useful tool to model random field $\mathcal{H}(\mathbf{x}, \theta)$. The traditional way of dealing with random field is to discretize the random field into finite number of random variables. The available schemes for discretizing random fields can be broadly divided into three groups: point discretization (e.g., midpoint method [40], shape function method [47,48], integration point method [55], optimal linear estimate method [43]); average discretization method (e.g., spatial average [85,86], weighted integral method [15,16]), and series expan-

sion method (e.g., orthogonal series expansion [91]). An advantageous alternative for discretizing $\mathcal{H}(\mathbf{x}, \theta)$ is to represent it in a generalized Fourier type of series as, often termed as Karhunen–Loève (KL) expansion [39,51]. Suppose, $\mathcal{H}(\mathbf{x}, \theta)$ is a random field with covariance function $\Gamma_{\mathcal{H}}(\mathbf{x}_1, \mathbf{x}_2)$. The KL expansion for $\mathcal{H}(\mathbf{x}, \theta)$ takes the following form

$$\mathcal{H}(\mathbf{x}, \theta) = \bar{\mathcal{H}}(\mathbf{x}) + \sum_{i=1}^{\infty} \sqrt{\lambda_i} \xi_i(\theta) \psi_i(\mathbf{x}) \tag{81}$$

where $\{\xi_i(\theta)\}$ is a set of uncorrelated random variables. $\{\lambda_i\}$ and $\{\psi_i(\mathbf{x})\}$ are the eigenvalues and eigenfunctions of the covariance kernel $\Gamma_{\mathcal{H}}(\mathbf{x}_1, \mathbf{x}_2)$, satisfying the integral equation

$$\int_{\mathfrak{R}^N} \Gamma_{\mathcal{H}}(\mathbf{x}_1, \mathbf{x}_2) \psi_i(\mathbf{x}_1) d\mathbf{x}_1 = \lambda_i \psi_i(\mathbf{x}_2) \tag{82}$$

In practise, the infinite series of Eq. (81) must be truncated, yielding a truncated KL approximation

$$\bar{\mathcal{H}}(\mathbf{x}, \theta) \cong \bar{\mathcal{H}}(\mathbf{x}) + \sum_{i=1}^{M} \sqrt{\lambda_i} \xi_i(\theta) \psi_i(\mathbf{x}) \tag{83}$$
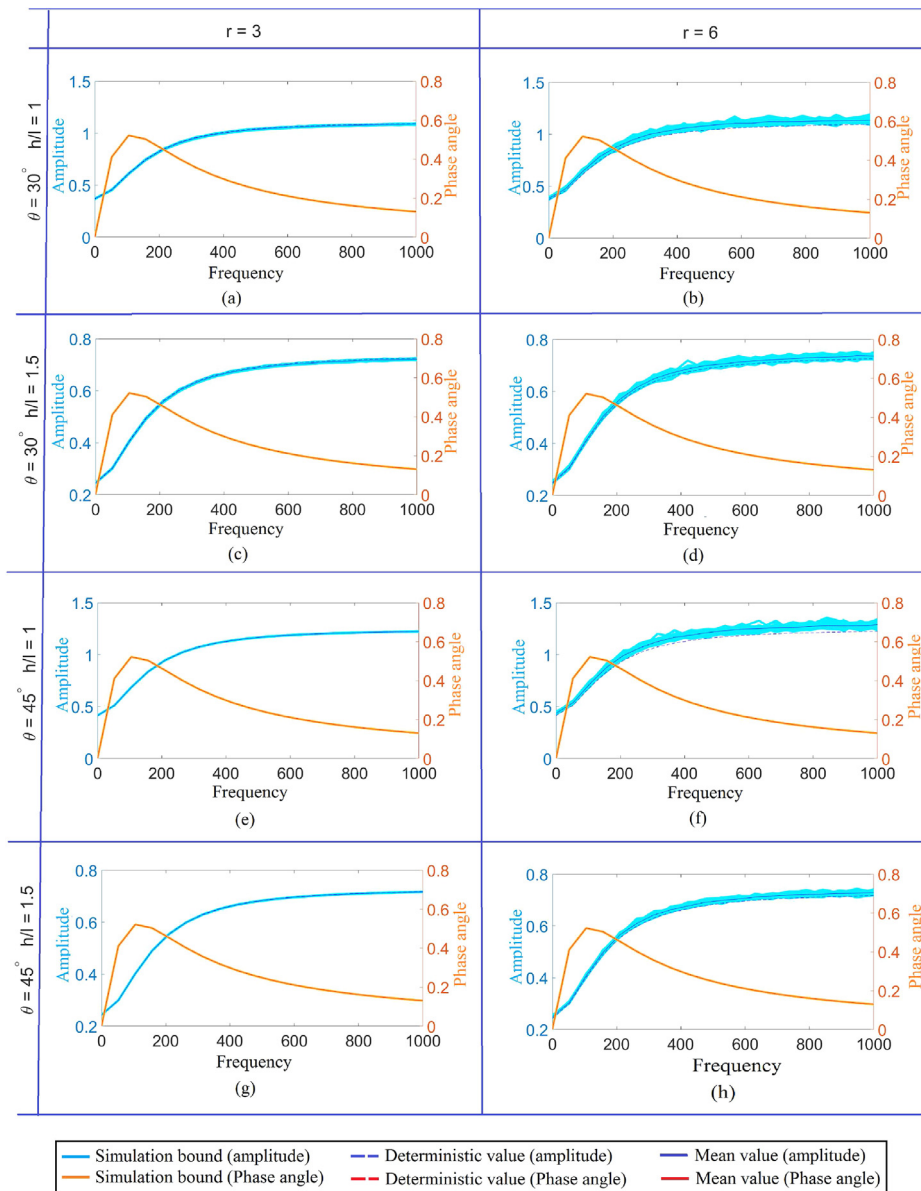
Fig. 17. Effect of viscoelasticity on shear modulus G_{12} corresponding to randomly correlated inhomogeneous lattices having spatial structural irregularity. Frequency dependent amplitudes and phase angles are presented for various cellular configurations considering two different degree of structural irregularity ($r = 3$ and $r = 6$).

which approaches $\mathcal{H}(\mathbf{x}, \theta)$ in the mean square sense as the positive integer $M \to \infty$. Finite element methods can be readily applied to obtain eigensolutions of any covariance function and domain of the random field. For linear or exponential covariance functions and simple domains, the eigensolutions can be evaluated analytically [26,33]. Once $\Gamma_{\mathcal{H}}(\mathbf{x}_1, \mathbf{x}_2)$ and its eigensolutions are determined, the parameterization of $\tilde{\mathcal{H}}(\mathbf{x}, \theta)$ is achieved by the KL approximation of its Gaussian image, i.e.,

$$\tilde{\mathcal{H}}(\mathbf{x}, \theta) \cong G \left[\bar{\mathcal{H}}(\mathbf{x}) + \sum_{i=1}^{M} \sqrt{\lambda_i} \xi_i(\theta) \psi_i(\mathbf{x}) \right] \qquad (84)$$

According to Eq. (84), the KL approximation provides a parametric representation of the random field $\mathcal{H}(\mathbf{x}, \theta)$. It is to be noted that KL expansion is not the only available discretization scheme for the random field $\mathcal{H}(\mathbf{x}, \theta)$. However, KL expansion has some desirable properties, such as uniqueness and error-minimization, making it a convenient choice over other available methods. The readers may refer to [26,33] for a detailed study of the cited and other KL expansion properties.

In the present study, both intrinsic material properties and structural irregularity are represented as random fields and discretized using the KL expansion with a Gaussian random field. For both the cases, the covariance function is assumed to be represented as:

$$\Gamma_{\mathcal{H}}(y_1, z_1; y_2, z_2) = \sigma_{\mathcal{H}}^2 e^{(-|y_1 - y_2|/b_y) + (-|z_1 - z_2|/b_z)} \qquad (85)$$

in which b_y and b_z are the correlation parameters along y and z directions (that corresponds to direction - 1 and direction - 2 respectively, as shown in Fig. 1(b)) and where $\sigma_{\mathcal{H}}^2$ is the variance of the random field. These quantities control the rate at which the covariance decays. In a two dimensional physical space the eigensolutions of the covariance function are obtained by solving the integral equation (refer to Eq. (82)) analytically

$$\lambda_i \psi_i(y_2, z_2) = \int_{-a_1}^{a_1} \int_{-a_2}^{a_2} \Gamma_{\mathcal{H}}(y_1, z_1; y_2, z_2) \psi_i(y_1, z_1) \, dy_1 \, dz_1 \qquad (86)$$

where $-a_1 \leqslant y \leqslant a_1$ and $-a_2 \leqslant z \leqslant a_2$. Substituting the covariance function and assuming the eigen-solution is separable in y and z directions,

Fig. 18. Probability density function plots for the amplitude of the elastic moduli considering randomly inhomogeneous form of stochasticity for different structural configurations and degree of structural irregularity ($r = 3$ and $r = 6$). Results are presented for the three in-plane elastic moduli as a ratio of the values corresponding to irregular configurations and respective deterministic values. Probabilistic descriptions are shown both at a lower frequency (100 Hz) and a relatively higher frequency (800 Hz).

i.e.

$$\psi_i(y_2, z_2) = \psi_i^{(y)}(y_2)\psi_i^{(z)}(z_2) \qquad (87)$$

$$\lambda_i(y_2, z_2) = \lambda_i^{(y)}(y_2)\lambda_i^{(z)}(z_2) \qquad (88)$$

The solution of Eq. (86) reduces to the product of the solutions of two equations of the form

$$\lambda_i^{(y)}\psi_i^{(y)}(y_1) = \int_{-a_1}^{a_1} e^{(-|y_1-y_2|/b_y)}\psi_i^{(y)}(y_2)dy_2 \qquad (89)$$

The solution of this equation, which is the eigensolution (eigenvalues and eigenfunctions) of an exponential covariance kernel for a one-

dimensional random field is obtained as

$$\begin{cases} \psi_i(\zeta) = \dfrac{\cos(\omega_i\zeta)}{\sqrt{a + \frac{\sin(2\omega_i a)}{2\omega_i}}} & \lambda_i = \dfrac{2\sigma_H^2 b}{\omega_i^2 + b^2} & \text{for } i \text{ odd} \\[3ex] \psi_i(\zeta) = \dfrac{\sin(\omega_i^*\zeta)}{\sqrt{a - \frac{\sin(2\omega_i^* a)}{2\omega_i*}}} & \lambda_i^* = \dfrac{2\sigma_H^2 b}{\omega_i^{*2} + b^2} & \text{for } i \text{ even} \end{cases} \qquad (90)$$

where $b = 1/b_y$ or $1/b_z$ and $a = a_1$ or a_2. ζ can be either y or z; ω_i and ω_i^* are the solutions of equations $b - \omega_i \tan(\omega_i a) = 0$ and $\omega_i + b\tan(\omega_i a) = 0$ respectively. It is to be noted that the KL expansion was developed for discretizing Gaussian random fields and hence, all the operations described above are only applicable to Gaussian random fields. For lognormal random fields considered in this study, the KL expansion is carried out on its classical Gaussian image.

In the present analysis of spatially irregular lattices with spatially varying viscoelastic properties, the scheme for introducing structural ir-
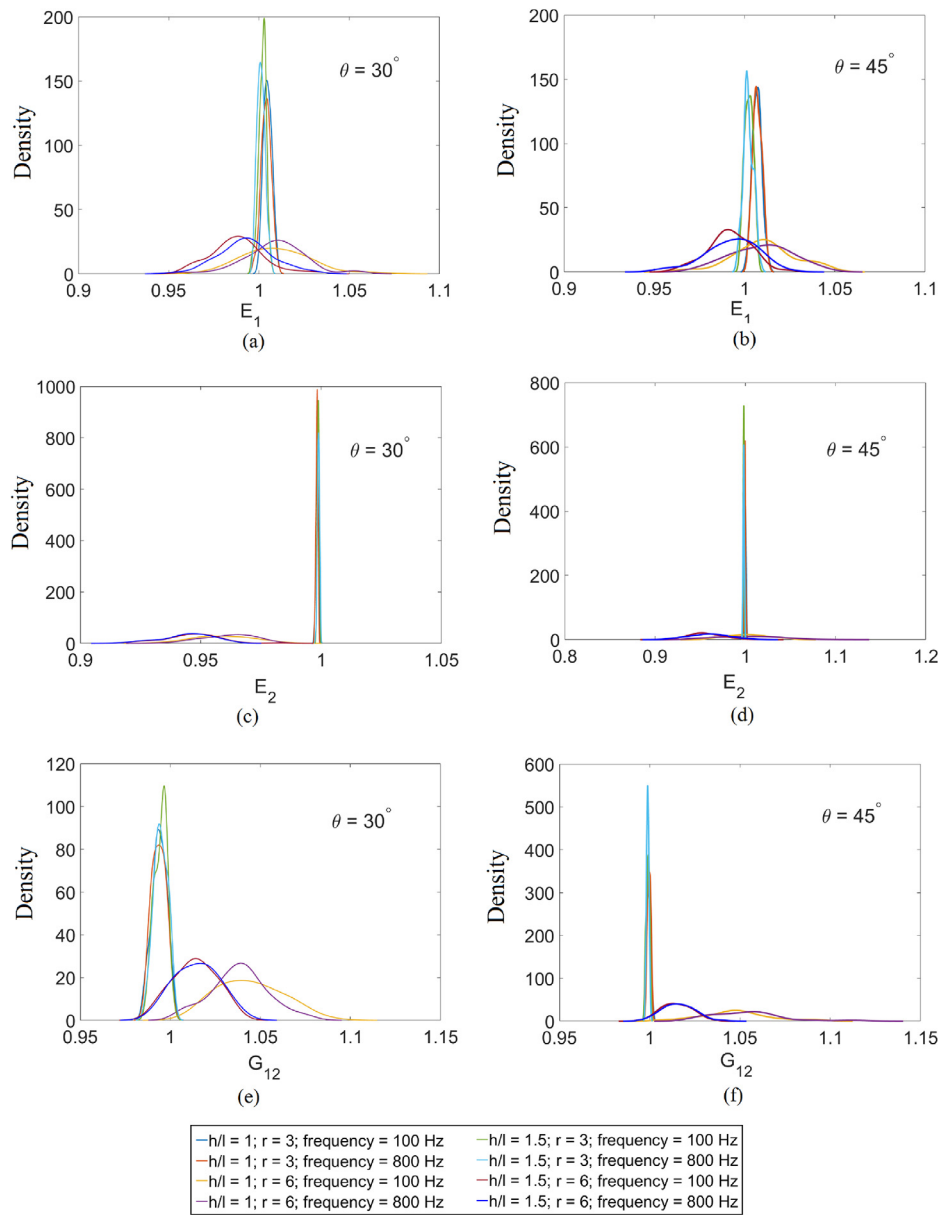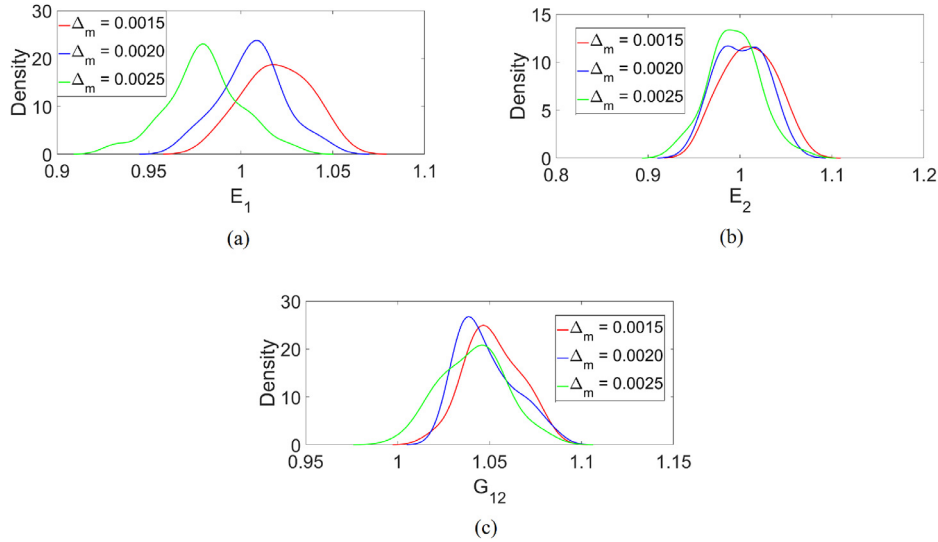
Fig. 19. Probability density function plots for the amplitude of the elastic moduli considering randomly inhomogeneous form of stochasticity for different values of Δ_m (i.e. coefficient of variation for spatially random correlated material properties, such as E_s, μ and ϵ). Results are presented as a ratio of the values corresponding to irregular configurations and respective deterministic values (for a frequency of 800 Hz).

regularity is explained in Fig. 1(a), where it can be noticed that each node of a regular lattice is simultaneously perturbed with a certain bound (defined by degree of irregularity) for each of the realizations [62]. A typical resulting structure obtained from Fig. 1(a) after introducing irregularity is shown in Fig. 1(b). Multiple such structural configurations with random geometry are considered to quantify the effect of irregularity. Each structural parameter and each material parameter is represented by an independent random field parametrized by a mean value, a coefficient of variation (ratio of the mean value and the standard deviation) and two correlation parameters. The mean values are equal to the deterministic nominal values. To present the results in a physically insightful way for randomly inhomogeneous systems, we have defined (1) a unique degree of structural irregularity (r) and (2) a unique degree of material property variation (Δ_m). The two parameters are equal to the respective coefficients of variation of their Gaussian random fields. The statistical results are computed on the basis of 10,000 such realizations of irregular lattices.

5. Results and discussion

In this section results are presented to portray the viscoelastic effect on effective in-plane material properties of irregular hexagonal lattices considering two different forms of irregularity in structural and material attributes: randomly inhomogeneous correlated irregularity and randomly homogeneous irregularity [71]. In randomly inhomogeneous correlated system, spatial variability of the stochastic structural attributes are accounted, wherein each sample of the Monte Carlo simulation includes the spatially random distribution of structural and materials attributes with a rule of correlation. The spatial variability in structural and material properties (E_s, μ and ϵ) are physically attributed by degree of structural irregularity (r) and degree of material property variation (Δ_m) respectively, as discussed in the Section 4. In randomly homogeneous system, no spatial variability is considered. It is assumed that structural and material attributes remain the same spatially for a particular realization. However the stochastic parameters vary from sample to sample following a probabilistic distribution (a Monte Carlo simulation based random variable approach). This model of irregularity can be regarded as a random distribution of over and under expanded cells. The degree of stochasticity in randomly homogeneous system (r) is defined based on the coefficient of variation of the considered random distribution. As the two Young's moduli and shear modulus for low den-

sity lattices are proportional to $E_s \rho^3$ [92], the non-dimensional results for in-plane elastic moduli E_1, E_2, v_{12}, v_{21} and G_{12}, unless otherwise mentioned, are presented as: $\bar{E}_1 = \dfrac{E_{1eq}}{E_s \rho^3}$, $\bar{E}_2 = \dfrac{E_{2eq}}{E_s \rho^3}$, $\bar{v}_{12} = v_{12eq}$, $\bar{v}_{21} = v_{21eq}$ and $\bar{G}_{12} = \dfrac{G_{12eq}}{E_s \rho^3}$ respectively, where ' $(\bar{\cdot})$ ' denotes the non-dimensional elastic modulus and ρ is the relative density of the lattice (defined as a ratio of the planar area of solid to the total planar area of the lattice) (Fig. 6).

5.1. Analysis of spatially correlated irregular lattices without considering viscoelasticity

As discussed in the Section 3, the two Young's moduli and shear modulus depend on the viscoelastic intrinsic material properties of the constituent members, while the two Poisson's ratios depend only on the structural configurations. For this reason, we have concentrated primarily on the two Young's moduli and shear modulus to show the viscoelastic effect. However, the variation of all the in-plane elastic moduli for spatially correlated structural randomness are presented without considering the effect of viscoelasticity in Figs. 3–5 (obtained using Eqs. (19)–(23)). The results are compared with the elastic moduli obtained from direct finite element simulation. The elastic moduli are obtained for two different h/l ratios (1 and 1.5) considering different cell angles $\theta = 30°$ and $\theta = 45°$ with a small t/l value ($\sim 10^{-2}$) corresponding to respective deterministic lattice configurations (refer Fig. 1(d)).

The elastic moduli of hexagonal lattices with spatially correlated structural irregularities are found (refer to Figs. 3–5) to be increasingly influenced for higher degree of structural irregularity (r) causing a significant change in the respective mean values with a wide response bound. Such inevitable variability in the responses make it crucial to account for the effect of system irregularity in the analysis and design of hexagonal lattices. It can be noticed from Figs. 3–5 that the elastic moduli obtained using the analytical formulae and the direct finite element simulation are in good agreement corroborating the validity of the analytical formulae for spatially correlated structural randomness. Fig. 8 shows the variation of effective normalized relative density (normalized with respect to the corresponding relative density of regular structural configurations) for irregular lattices considering different structural configurations with increasing degree of spatially correlated structural irregularity. The figure reveals an interesting in-
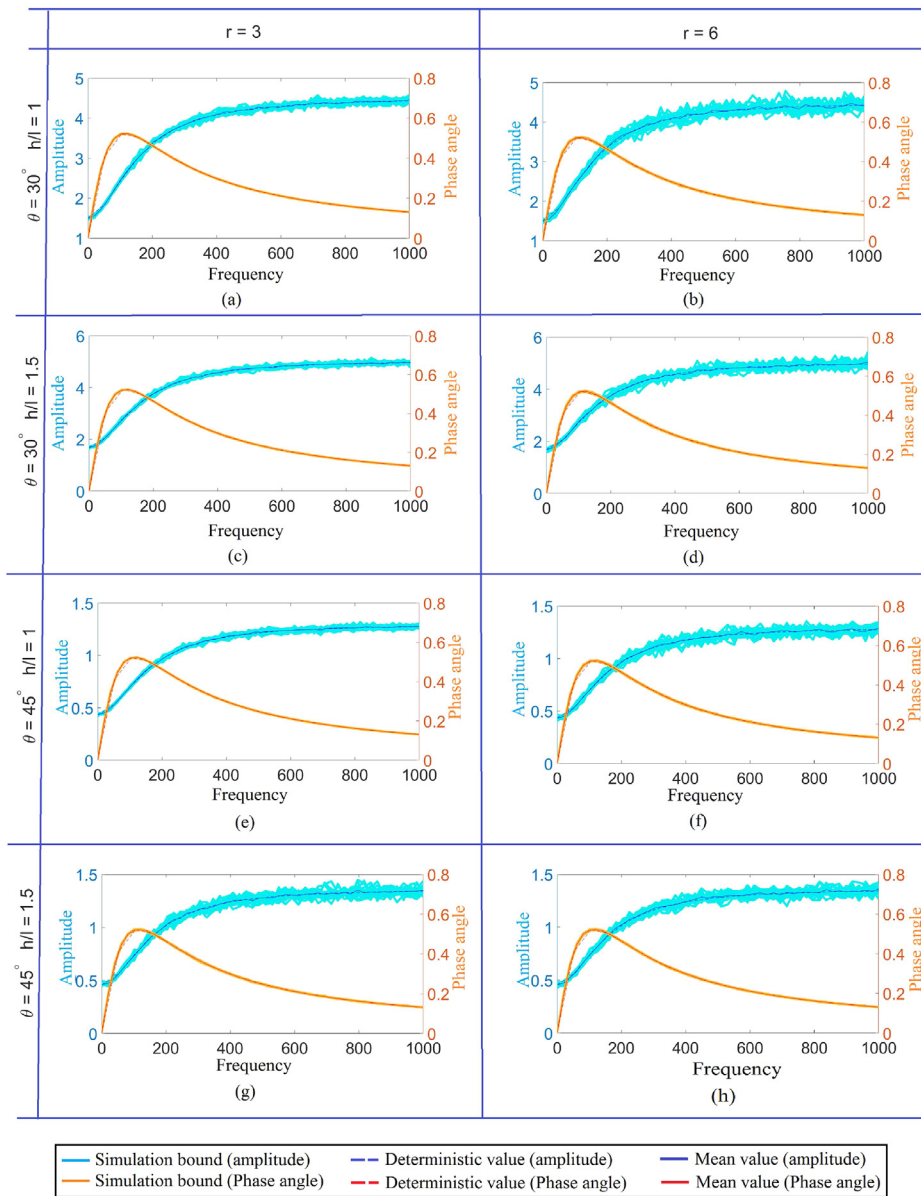
Fig. 20. Effect of viscoelasticity on elastic modulus E_1 considering randomly homogeneous form of stochasticity in the structural and material attributes. Frequency dependent amplitudes and phase angles are presented for various cellular configurations considering two different degree of stochasticity ($r = 3$ and $r = 6$).

formation; even though a regular hexagonal lattice with $\theta = 30°$ and $h/l = 1$ is regarded as the most efficient space filling pattern in a two dimensional space, this structural configuration gets the most affected by spatial irregularity. Influence of irregularity on the structural configuration with $h/l = 1$ is noticed to be higher than the $h/l = 1.5$ configuration for both the cell angles (θ) (Fig. 7) .

5.2. Deterministic analysis for the viscoelastic properties of regular lattices

Deterministic results depicting the effect of viscoelasticity on the two Young's moduli and the shear modulus of regular hexagonal lattices are presented in Figs. 9–11. The amplitude gives an impression about the strength of the frequency components relative to other components (i.e. frequency of the constituting signals corresponding to different amplitudes of the conventional time domain representation), while the phase shows how all the frequency components align in time. Fig. 9 shows the variation of amplitude and phase angle with frequency for the three viscoelastic moduli considering different lattice configurations. To obtain numerical results we have considered the viscoelastic parameters

$\mu = \omega_{max}/5$ (where ω_{max} is the maximum value of considered frequency) and $\epsilon = 2$. With increasing value of frequency the amplitude of elastic moduli are found to increase until a limit elastic moduli as explained in Eq. (18). For very low frequency (i.e. $\omega \rightarrow 0$), amplitude of all the three moduli assume the value of classical elastic moduli as provided by [27]. Similar trend has been reported for the viscoelastic properties of strand-based composites in time domain [54]. The expressions provided by [27] for accounting viscoelastic effect of honeycombs in time domain also yield similar results. Fig. 9 also shows the variation of phase angle for the three elastic moduli with frequency. However, as the phase angles corresponding to the Young's moduli and shear modulus for regular lattices are same as the phase angle of the complex intrinsic elastic material property of the lattice, the numerical values are indifferent for various structural configurations and they are also same for the different elastic moduli (refer to Eq. (58)). A peak value of the phase angle is observed for a certain critical frequency in all the tree cases. This behaviour can be explained by the use of a Biot model here which is equivalent to the standard linear model represented in Fig. 2(c): for very low and very large frequencies, the model behaves like pure elastic
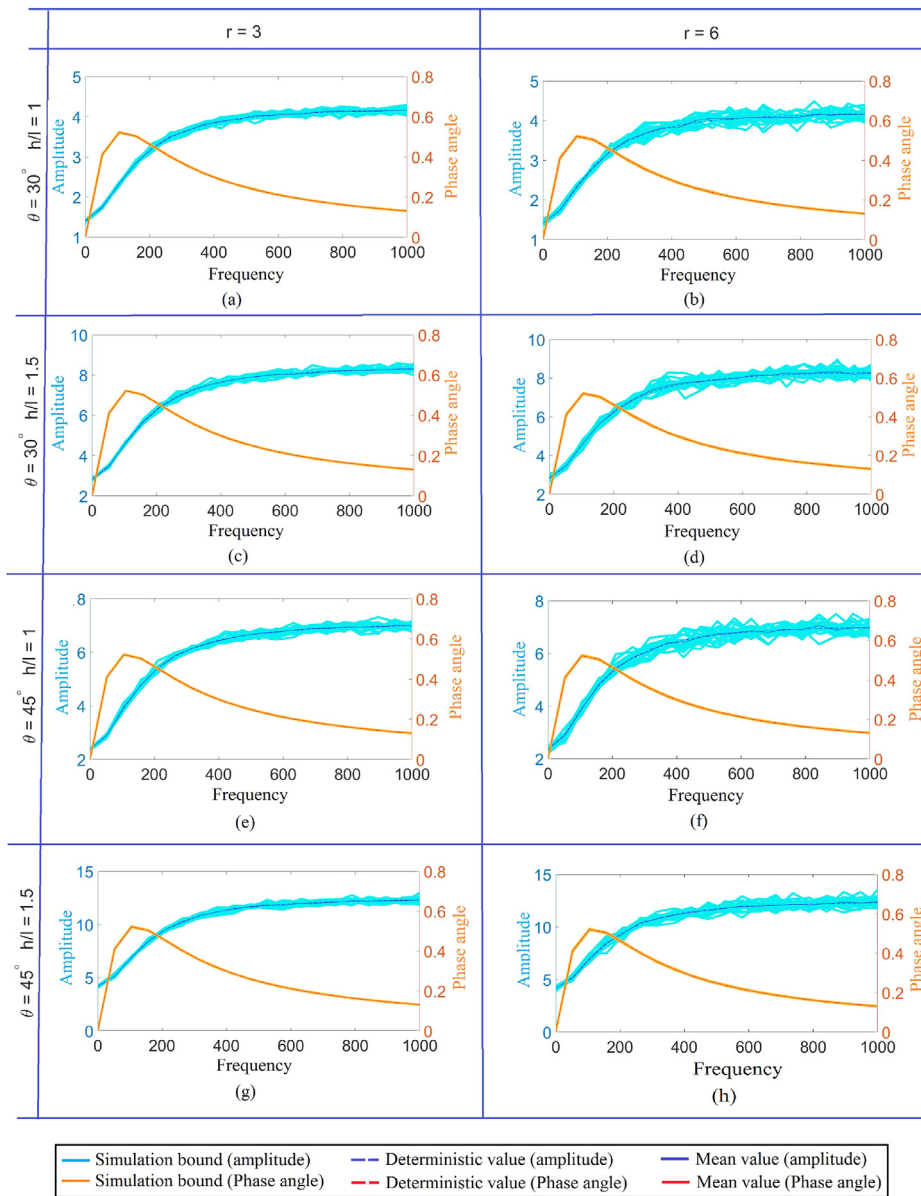
Fig. 21. Effect of viscoelasticity on elastic modulus E_2 considering randomly homogeneous form of stochasticity in the structural and material attributes. Frequency dependent amplitudes and phase angles are presented for various cellular configurations considering two different degree of stochasticity ($r = 3$ and $r = 6$).

while near the critical frequency (which can easily be calculated using Eq. (14)) the viscous effect induced by the dashpot is maximum and for very large values of ϵ, the phase at the critical frequency tend to $\pi/2$ which corresponds to a pure viscous effect. Unlike amplitude of the elastic moduli, it is interesting to notice that the variation of phase angle with frequency does not depend on the lattice configuration for regular lattices, as discussed in Section 3.6.

Fig. 10(a) and (b) show the effect of variation of the viscoelastic parameters μ and ϵ respectively on the amplitude of the elastic moduli with regular structural configuration, while Fig. 11(a) and (b) show the effect of viscoelasticity for the phase angles of elastic moduli. Normalized values (with respect to the corresponding elastic modulus for $\omega = 0$) of the elastic moduli, as shown in the Y-axes of the figures, are presented for the purpose of comparison. It is evident from the figure that μ and ϵ influence the factor of amplification for the amplitude and phase angle of the elastic moduli. As the results in Figs. 10 and 11 are presented in the form of non-dimensional ratios normalized by respective elastic modulus, these observations are valid for all the three viscoelastic moduli (i.e. E_1, E_2 and G_{12}). It is interesting to notice from Figs. 10 and

11 that μ controls the critical frequency value (the critical frequency value increases with the increase of μ), while ϵ controls the value of peak amplitude as well as phase angle of the elastic moduli (the peak values of amplitude and phase angle decrease with the increase of ϵ).

5.3. Analysis of the viscoelastic properties for spatially correlated irregular lattices with randomly inhomogeneous form of irregularity

Scope of the present investigation includes the compound effect of viscoelasticity and irregularity of the lattices. Results corresponding to randomly inhomogeneous correlated structural and material irregularity are presented in this subsection, followed by randomly homogeneous structural and material irregularity in the next subsection.

There are two different types of randomness (related to structural and material attributes) involved in the present problem of viscoelastic lattices with spatially varying system parameters. One is random variation of the X- and Y- coordinates of the joints (within a circular bound, which defines the degree of irregularity) with respect to their corresponding deterministic values, as shown in Fig. 1(a). The random vari-
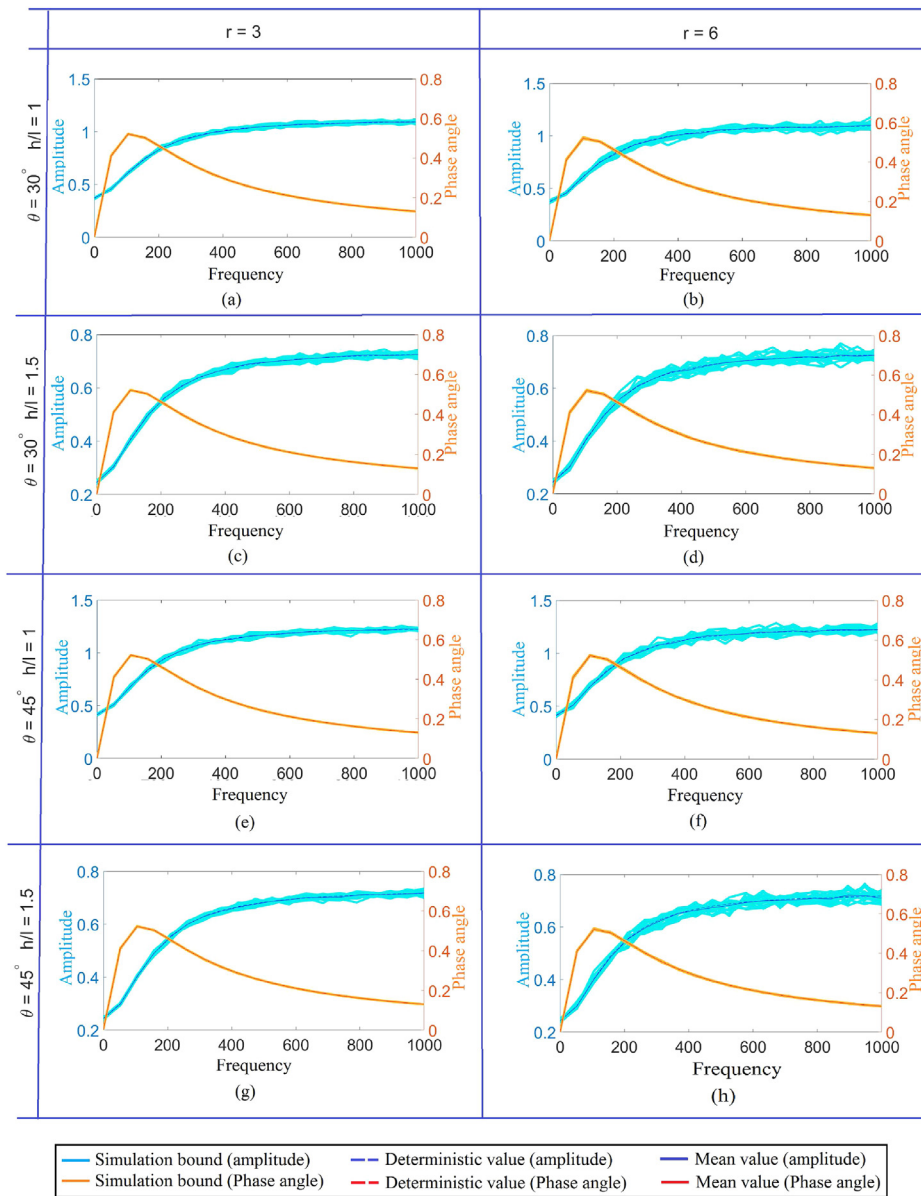
Fig. 22. Effect of viscoelasticity on shear modulus G_{12} considering randomly homogeneous form of stochasticity in the structural and material attributes. Frequency dependent amplitudes and phase angles are presented for various cellular configurations considering two different degree of stochasticity ($r = 3$ and $r = 6$).

ation of X- and Y- coordinates are considered to be correlated spatially while generating the respective deviated values. A Gaussian random field is used for this purpose following the standard approach described in Section 4. In case of material properties (such as intrinsic Young's modulus and viscoelastic parameters), correlated spatial randomness is imposed on each unit cell as shown in Fig. 1(e). Similar to the case of spatially random structural irregularity, a Gaussian random field is used to model the correlated material properties of each constituting unit cell of the lattice. Representative plots showing the typical distribution of correlated structural and material attributes are shown in Fig. 12 for a particular realization. Multiple such random realizations (following a Gaussian random field) are considered in this paper to present the results in a probabilistic framework. Fig. 13 presents the structural configuration of a hexagonal lattice with different degree of structural irregularities considering a single random realization, while Fig. 14 shows the simulation bound an irregular hexagonal lattice for multiple random realizations considering $\theta = 30°$, $h/l = 1$ and $r = 6$. These figures provide a physical perspective of the correlated structural randomness considered in this study.

The compound effect of spatially correlated structural and material irregularity on the viscoelastic material properties of hexagonal lattices (randomly inhomogeneous system) are presented in Figs. 15–17 for two different degree of structural irregularities (with $\Delta_m = 0.002$) considering various structural configurations. The response bounds, mean values and deterministic values of the amplitude and phase angles are shown corresponding to various frequencies. It is observed that the response bounds increase with increasing degree of structural irregularity (r), as expected. The response bounds for the elastic moduli also increase with the increasing value of frequency and then becomes constant as the mean value becomes constant. However, it is interesting to notice that the variation of phase angle with frequency is least influenced by the spatially random structural and material irregularity in the system. Besides that, the phase angle also remain independent of the deterministic lattice configuration under consideration. Probabilistic descriptions for the variation of the amplitudes of viscoelastic properties are shown in Fig. 18 for both lower and higher frequency ranges, wherein it can be noticed that the elastic moduli follow a Gaussian distribution. The effect for variation of the degree of stochasticity in spatially random intrinsic
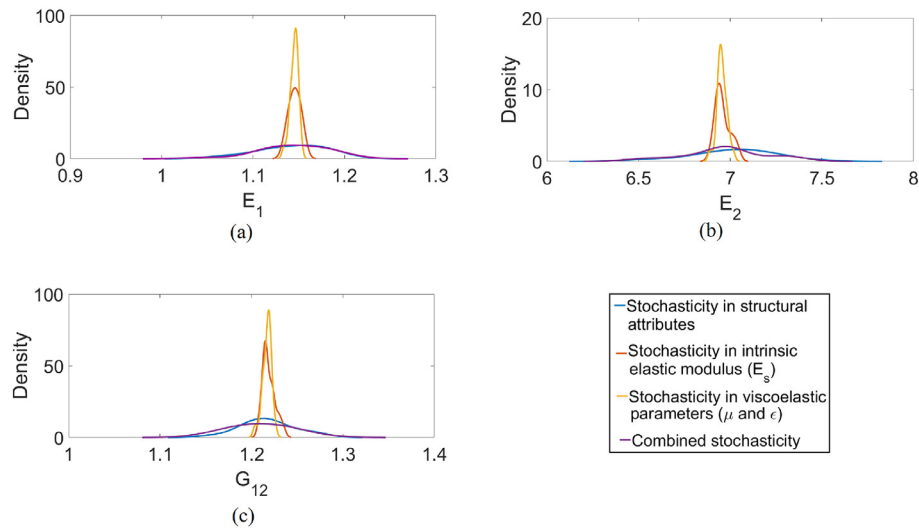
Fig. 23. Probabilistic descriptions for the amplitudes of three effective viscoelastic properties corresponding to a frequency of 800 Hz considering individual and compound effect of stochasticity in material and structural attributes with $r = 6$.

material properties and viscoelastic parameters (Δ_m) is investigated considering a lattice configuration with $\theta = 45°$ and $h/l = 1$ corresponding to a frequency of 800 Hz. From the probability distributions depicted in Fig. 19, it is observed that the response bound and the mean value increase and decrease respectively with the increasing value of Δ_m.

5.4. Analysis of the viscoelastic properties for randomly homogeneous form of structural and material irregularities

The amplitude and phase angle of viscoelastic properties considering randomly homogeneous form of structural and material irregularities are presented in Figs. 20–22. In case of randomly homogeneous irregularity, coefficient of variation (COV) of the samples for a particular parameter ($r = 1000 \times$COV) is defined to relate degree of irregularity with the results. The elastic moduli are obtained considering a compound effect of various structural (h, l and θ) and material attributes (E_s, μ, ϵ) for different degree of stochasticity (r). From the figures, the viscoelastic response bounds for amplitudes are found to increase with increasing degree of irregularity, as expected. Similar to the case of randomly inhomogeneous irregularity, the response bounds for the elastic moduli also increase with the increasing value of frequency and then becomes constant. Even though the results obtained for the two different forms of irregularities (randomly inhomogeneous and randomly homogeneous) are not directly comparable, it is interesting to notice that the difference between deterministic values and response mean for the amplitude of effective viscoelastic properties are negligible in case of randomly homogeneous irregularity, while there exists a significant difference between these two parameters in case of randomly inhomogeneous irregularity. Variation of phase angle with frequencies shows a similar trend like randomly inhomogeneous system, wherein a negligible variability in the response bound is observed. Fig. 23 presents the probabilistic distributions for the two Young's moduli and the shear modulus (with a frequency of 800 Hz) considering individual and combined effect of structural and material irregularity. The results are shown considering a lattice configuration with $\theta = 45°$ and $h/l = 1$. From the response bounds corresponding to different probability distributions, it can be discerned that the structural irregularity has the most influential effect on the amplitude of effective viscoelastic properties for randomly homogeneous irregular lattices. This result could be expected regarding Eqs. (77) and (78) where the structural parameters have a power of three while material and viscoelastic parameters have lesser powers.

6. Conclusion

The effect of viscoelasticity on irregular hexagonal lattices is investigated in frequency domain considering two different forms of irregularity in structural and material parameters, randomly inhomogeneous irregularity and randomly homogeneous irregularity. Practically relevant spatially correlated structural and material attributes are considered to account for the effect of randomly inhomogeneous form of irregularity based on Karhunen–Loève expansion. Closed-form analytical expressions are developed to quantify the effect of viscoelasticity for irregular lattices, wherein it is observed that the two Young's moduli and shear modulus are dependent on the viscoelastic parameters. Limiting values of the amplitude and phase angles are established based on the analytical framework. The two in-plane Poisson's ratios depend only on structural geometry of the lattice structure. Results are presented in both deterministic and stochastic regime to comprehensively analyse the structural behaviour. The amplitude of in-plane Young's moduli and shear modulus are amplified significantly due to the viscoelastic effect. Structural and material irregularity in the lattices cause considerable amount of variation in the amplitude of effective elastic moduli from their respective deterministic values, while the phase angle experiences negligible variation due to this.

Since the structural and material irregularities in lattices are inevitable for practical purposes and many of the common materials show viscoelastic behaviour in room temperature, the combined effect presented in this study will serve as a practical reference for future applications. Moreover, the developed analytical approach being computationally efficient, can be quite attractive for the purpose of analysis and design of lattices and metamaterials considering structural irregularities and the effect of viscoelasticity along with Monte Carlo simulation based reliability analysis of the system.

Acknowledgements

References

[1] Adhikari S. Energy dissipation in vibrating structures. Cambridge, UK: Cambridge University Engineering Department; 1998. First Year Report.

[2] Adhikari S, Woodhouse J. Identification of damping: part 1, viscous damping. J Sound Vibr 2001;243(1):43–61.

[3] Ajdari A, Jahromi BH, Papadopoulos J, Nayeb-Hashemi H, Vaziri A. Hierarchical honeycombs with tailorable properties. Int J Solids Struct 2012;49(11-12): 1413–1419.

[4] Ajdari A, Nayeb-Hashemi H, Canavan P, Warner G. Effect of defects on elastic-plastic behavior of cellular materials. Mater Sci Eng 2008;487(1-2):558–67.

[5] Bagley RL, Torvik PJ. Fractional calculus–a different approach to the analysis of viscoelastically damped structures. AIAA J 1983;21(5):741–8.

[6] Berinskii I. Elastic networks to model auxetic properties of cellular materials. Int J Mech Sci 2016;115–116:481–8.

[7] Berkache K, Deogekar S, Goda I, Picu R, Ganghoffer J-F. Construction of second gradient continuum models for random fibrous networks and analysis of size effects. Comp Struct 2017. doi:10.1016/j.compstruct.2017.08.078.

[8] Biot MA. Variational principles in irreversible thermodynamics with application to viscoelasticity. Phys Rev 1955;97(6):1463–9.

[9] Biot MA. Linear thermodynamics and the mechanics of solids. In: Proceedings of the Third U. S. National Congress on Applied Mechanics. New York: ASME; 1958. p. 1–18.

[10] Bland DR. Theory of linear viscoelasticity. London: Pergamon Press; 1960.

[11] Chen DH, Yang L. Analysis of equivalent elastic modulus of asymmetrical honeycomb. Comp Struct 2011;93(2):767–73.

[12] Christensen R. Theory of viscoelasticity: an introduction. Elsevier; 2012.

[13] Christensen RM. Theory of viscoelasticity. first. New York: Academic Press Inc; 1982. Reprinted by Dover Publication Inc, 2003, second Editon.

[14] Critchley R, Corni I, Wharton JA, Walsh FC, Wood RJK, Stokes KR. A review of the manufacture, mechanical properties and potential applications of auxetic foams. Physica Status Solidi B 2013;250(10):1963–82.

[15] Deodatis G. The weighted integral method, I: stochastic stiffness matrix. J Eng Mech-ASCE 1991;117(8):1851–64.

[16] Deodatis G, Shinozuka M. The weighted integral method, II : response variability and reliability. J Eng Mech-ASCE 1991;117(8):1865–77.

[17] Dey S, Mukhopadhyay T, Adhikari S. Metamodel based high-fidelity stochastic analysis of composite laminates: a concise review with critical comparative assessment. Comp Struct 2017;171:227–50.

[18] Dey S, Mukhopadhyay T, Naskar S, Dey T, Chalak H, Adhikari S. Probabilistic characterisation for dynamics and stability of laminated soft core sandwich plates. J Sandwich Struct Mater 2018. doi:10.1177/1099636217694229.

[19] Dey S, Mukhopadhyay T, Sahu S, Adhikari S. Effect of cutout on stochastic natural frequency of composite curved panels. Comp Part B 2016;105:188–202.

[20] Dey S, Mukhopadhyay T, Spickenheuer A, Adhikari S, Heinrich G. Bottom up surrogate based approach for stochastic frequency response analysis of laminated composite plates. Comp Struct 2016;140:712–27.

[21] Dey S, Mukhopadhyay T, Spickenheuer A, Gohs U, Adhikari S. Uncertainty quantification in natural frequency of composite plates: an artificial neural network based approach. Ad Comp Lett 2016;25:43–8.

[22] Dey S, Naskar S, Mukhopadhyay T, Gohs U, Spickenheuer A, Bittrich L, et al. Uncertain natural frequency analysis of composite plates including effect of noise – a polynomial neural network approach. Comp Struct 2016;143:130–42.

[23] El-Sayed FKA, Jones R, Burgess IW. A theoretical approach to the deformation of honeycomb based composite materials. Composites 1979;10(4):209–14.

[24] Enelund M, Olsson P. Damping described by fading memory–analysis and application to fractional derivative models. Int J Solids Struct 1999;36(7):939–70.

[25] Fung YC. Foundations of solid mechanics. Englewood Cliffs, New Jersey: Prentice-Hall Inc.; 1965.

[26] Ghanem R, Spanos P. Stochastic finite elements: a spectral approach. New York, USA: Springer-Verlag; 1991.

[27] Gibson L, Ashby MF. Cellular solids structure and properties. Cambridge, UK: Cambridge University Press; 1999.

[28] Golla DF, Hughes PC. Dynamics of viscoelastic structures - a time domain finite element formulation. Trans ASME, J Appl Mech 1985;52:897–906.

[29] Gonella S, Ruzzene M. Analysis of in-plane wave propagation in hexagonal and re-entrant lattices. J Sound Vibr 2008;312(1 - 2):125–39.

[30] Gonella S, Ruzzene M. Homogenization and equivalent in-plane properties of two-dimensional periodic lattices. Int J Solids Struct 2008;45(10):2897–915.

[31] Goswami S. On the prediction of effective material properties of cellular hexagonal honeycomb core. J Reinf Plast Comp 2006;25(4):393–405.

[32] Hu LL, Yu TX. Mechanical behavior of hexagonal honeycombs under low-velocity impact- theory and simulations. Int J Solids Struct 2013;50(20-21):3152–65.

[33] Huang SP, Quek ST, Phoon KK. Convergence study of the truncated karhunen-loeve expansion for simulation of stochastic processes. Int J Numer Methods Eng 2001;52:1029–43.

[34] Hurtado JE, Barbat AH. Monte carlo techniques in computational stochastic mechanics. Arch Comput Methods Eng 1998;5(1):3–29.

[35] Jang WY, Kyriakides S. On the buckling and crushing of expanded honeycomb. Int J Mech Sci 2015;91:81–90.

[36] Javid F, Liu J, Shim J, Weaver JC, Shanian A, Bertoldi K. Mechanics of instability-induced pattern transformations in elastomeric porous cylinders. J Mech Phys Solids 2016;96:1–17.

[37] Jimenez FL, Triantafyllidis N. Buckling of rectangular and hexagonal honeycomb under combined axial compression and transverse shear. Int J Solids Struct 2013;50(24):3934–46.

[38] Jones DIG. Handbook of viscoelastic vibration damping. Sussex, UK: Wiley-Blackwell; 2001.

[39] Karhunen K. Über lineare methoden in der wahrscheinlichkeitsrechnung. Annales Academiae Scientiarum Fennicae 1947;Ser. A137.

[40] Kiureghian AD. The stochastic finite element method in structural reliability. Probab Eng Mech 1988;3(2):83–91.

[41] Klintworth JW, Stronge WJ. Elasto-plastic yield limits and deformation laws for transversely crushed honeycombs. Int J Mech Sci 1988;30(3-4):273–92.

[42] Lesieutre GA, Mingori DL. Finite element modeling of frequency-dependent material properties using augmented thermodynamic fields. AIAA J Guidance, Control Dyn 1990;13:1040–50.

[43] Li C-C, Der Kiureghian A. Optimal discretization of random fields. J Eng Mech 1993;119(6):1136–54.

[44] Li K, Gao XL, Subhash G. Effects of cell shape and cell wall thickness variations on the elastic properties of two-dimensional cellular solids. Int J Solids Struct 2005;42(5):1777–95.

[45] Li K, Gao XL, Wang J. Dynamic crushing behavior of honeycomb structures with irregular cell shapes and non-uniform cell wall thickness. Int J Solids Struct 2007;44(14-15):5003–26.

[46] Liu Q, Mo Z, Wu Y, Ma J, Tsui GCP, Hui D. Crush response of cfrp square tube filled with aluminum honeycomb. Comp Part B 2016;98:406–14.

[47] Liu W, Belytschko T, Mani A. Probabilistic finite elements for nonlinear structural dynamics. Comput Methods Appl Mech Eng 1986;56(1):61–81.

[48] Liu W, Belytschko T, Mani A. Random field finite elements. Int J Numer Methods Eng 1986;23(10):1831–45.

[49] Liu W, Wang N, Huang J, Zhong H. The effect of irregularity, residual convex units and stresses on the effective mechanical properties of 2d auxetic cellular structure. Mater Sci Eng 2014;609:26–33.

[50] Liu Y, Xie B, Zhang Z, Zheng Q, Xu Z. Mechanical properties of graphene papers. J Mech Phys Solids 2012;60(4):591–605.

[51] Loève M. Probability theory. fouth. Springer-Verlag; 1977.

[52] Mahata A, Mukhopadhyay T, Adhikari S. A polynomial chaos expansion based molecular dynamics study for probabilistic strength analysis of nano-twinned copper. Mater Res Exp 2016;3(3):036501.

[53] Malek S, Gibson L. Effective elastic properties of periodic hexagonal honeycombs. Mech Mater 2015;91(1):226–40.

[54] Malekmohammadi S, Tressou B, Nadot-Martin C, Ellyin F, Vaziri R. Analytical micromechanics equations for elastic and viscoelastic properties of strand-based composites. J Comp Mater 2014;48(15):1857–74.

[55] Matthies HG, Brenner CE, Bucher CG, Guedes Soares C. Uncertainties in probabilistic numerical analysis of structures and solids-stochastic finite elements. Struct Safety 1997;19(3):283–336.

[56] McTavish DJ, Hughes PC. Modeling of linear viscoelastic space structures. Trans ASME, J Vibr Acoust 1993;115:103–10.

[57] Mousanezhad D, Ebrahimi H, Haghpanah B, Ghosh R, Ajdari A, Hamouda AMS, et al. Spiderweb honeycombs. Int J Solids Struct 2015. doi: http://dx.doi.org/10.1016/j.ijsolstr.2015.03.036.

[58] Mukhopadhyay T. A multivariate adaptive regression splines based damage identification methodology for web core composite bridges including the effect of noise. J Sandwich Struct Mater 2017. doi:10.1177/1099636216682533.

[59] Mukhopadhyay T, Adhikari S. Effective in-plane elastic properties of auxetic honeycombs with spatial irregularity. Mech Mater 2016;95:204–22.

[60] Mukhopadhyay T, Adhikari S. Equivalent in-plane elastic properties of irregular honeycombs: an analytical approach. Int J Solids Struct 2016;91:169–84.

[61] Mukhopadhyay T, Adhikari S. Free vibration analysis of sandwich panels with randomly irregular honeycomb core. J Eng Mech 2016. 10.1061/(ASCE)EM.1943-7889.0001153, 06010008.

[62] Mukhopadhyay T, Adhikari S. Effective in-plane elastic moduli of quasi-random spatially irregular hexagonal lattices. Int J Eng Sci 2017;119:142–79.

[63] Mukhopadhyay T, Adhikari S. Stochastic Mech of metamaterials. Comp Struct 2017;162:85–97.

[64] Mukhopadhyay T, Dey TK, Chowdhury R, Chakrabarti A, Adhikari S. Optimum design of frp bridge deck: an efficient rs-hdmr based approach. Struct Multidiscip Optim 2015;52(3):459–77.

[65] Mukhopadhyay T, Mahata A, Adhikari S, Zaeem MA. Effective elastic properties of two dimensional multiplanar hexagonal nano-structures. 2D Mater 2016. doi:10.1088/2053-1583/aa551c.

[66] Mukhopadhyay T., Mahata A., Adhikari S., Zaeem M.A. Effective mechanical properties of multilayer nano-heterostructures. Under review 2017.

[67] Mukhopadhyay T, Mahata A, Dey S, Adhikari S. Probabilistic analysis and design of hcp nanowires: an efficient surrogate based molecular dynamics simulation approach. J Mater Sci Technol 2016;32(12):1345–51.

[68] Mukhopadhyay T, Naskar S, Dey S, Adhikari S. On quantifying the effect of noise in surrogate based stochastic free vibration analysis of laminated composite shallow shells. Comp Struct 2016;140:798–805.

[69] Nady KE, Ganghoffer J. Computation of the effective mechanical response of biological networks accounting for large configuration changes. J Mech Behav Biomed Mater 2016;58:28–44.

[70] Nady KE, Reis FD, Ganghoffer J. Computation of the homogenized nonlinear elastic response of 2d and 3d auxetic structures based on micropolar continuum models. Comp Struct 2017;170:271–90.

[71] Naskar S, Mukhopadhyay T, Sriramula S, Adhikari S. Stochastic natural frequency analysis of damaged thin-walled laminated composite beams with uncertainty in micromechanical properties. Comp Struct 2017;160:312–34.

[72] Oftadeh R, Haghpanah B, Papadopoulos J, Hamouda A, Nayeb-Hashemi H, Vaziri A. Mech of anisotropic hierarchical honeycombs. Int J Mech Sci 2014;81:126–36.

[73] Pantano A, Parks DM, Boyce MC. Mechanics of deformation of single- and multi-wall carbon nanotubes. J Mech Phy Solids 2004;52(4):591–605.

[74] Papka SD, Kyriakides S. In-plane compressive response and crushing of honeycomb. J Mech Phy Solids 1994;42(10):1499–532.

[75] Papka SD, Kyriakides S. Experiments and full-scale numerical simulations of in-plane crushing of a honeycomb. Acta Materialia 1998;46(8):2765–76.

[76] Reis FD, Ganghoffer J. Construction of micropolar continua from the asymptotic homogenization of beam lattices. Comput Struct 2012;112:354–63.

[77] Reis FD, Ganghoffer J. Equivalent mechanical properties of auxetic lattices from discrete homogenization. Comput Mater Sci 2012;51(1):314–21.

[78] Reis FD, Ganghoffer J. Homogenized elastoplastic response of repetitive 2d lattice truss materials. Comput Mater Sci 2014;84:145–55.

[79] Reis FD, Ganghofferi J. Discrete homogenization of architectured materials: implementation of the method in a simulation tool for the systematic prediction of their effective elastic properties. Technische Mechanik 2010;30(1–3):85–109.

[80] Ronan W, Deshpande VS, Fleck NA. The tensile ductility of cellular solids: the role of imperfections. Int J Solids Struct 2016;102–103:200–13.

[81] Rouleau L, Dea J-F, Legay A, Lay FL. Application of kramers-kronig relations to time-temperature superposition for viscoelastic materials. Mech Mater 2013;65(10):66–75.

[82] Schaeffer M, Ruzzene M. Wave propagation in multistable magneto-elastic lattices. Int J Solids Struct 2015;56–57:78–95. http://dx.doi.org/10.1016/j.ijsolstr.2014.12.003.

[83] Srivastava A. Metamaterial properties of periodic laminates. J Mech Phy Solids 2016;96:252–63.

[84] Triantafyllidis N, Schraad MW. Onset of failure in aluminum honeycombs under general in-plane loading. J Mech Phy Solids 1998;46(6):1089–124.

[85] Vanmarcke E. Random fields: analysis and synthesis. Cambridge: World Scientific Publishing Co. Pte. Ltd.; 1983.

[86] Vanmarcke E, Grigoriu M. Stochastic finite-element analysis of simple beams. J Eng Mech-ASCE 1983;109(5):1203–14.

[87] Wilbert A, Jang WY, Kyriakides S, Floccari JF. Buckling and progressive crushing of laterally loaded honeycomb. Int J Solids Struct 2011;48(5):803–16.

[88] Yongqiang L, Zhiqiang J. Free flexural vibration analysis of symmetric rectangular honeycomb panels with scsc edge supports. Comp Struct 2008;83(2):154–8.

[89] Zenkert D. An introduction to sandwich construction. London: Chameleon Press; 1995.

[90] Zhang J, Ashby MF. The out-of-plane properties of honeycombs. Int J Mech Sci 1992;34(6):475–89.

[91] Zhang J, Ellingwood B. Orthogonal series expansion of random fields in reliability analysis. J Eng Mech-ASCE 1994;120(12):2660–77.

[92] Zhu HX, Hobdell JR, Miller W, Windle AH. Effects of cell irregularity on the elastic properties of 2d voronoi honeycombs. J Mech Phy Solids 2001;49(4):857–70.

[93] Zhu HX, Thorpe SM, Windle AH. The effect of cell irregularity on the high strain compression of 2d voronoi honeycombs. Int J Solids Struct 2006;43(5):1061–78.

[94] Zschernack C, Wadee MA, Vollmecke C. Nonlinear buckling of fibre-reinforced unit cells of lattice materials. Comp Struct 2016;136:217–28.